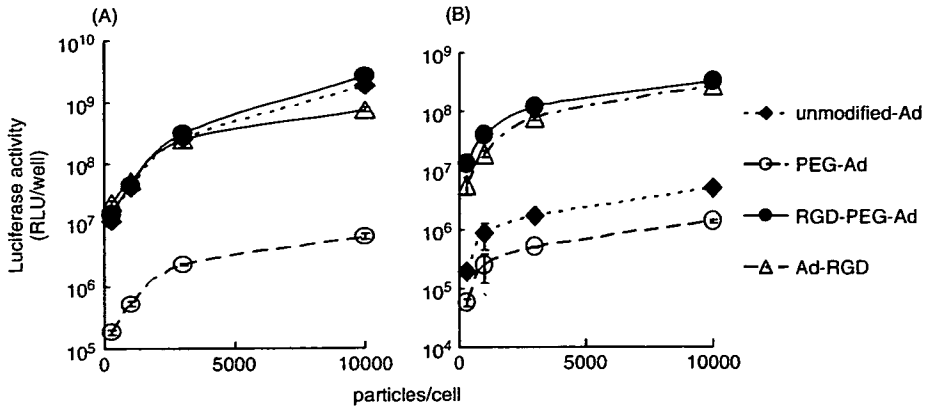

Figure 4. Transduction efficiency of RGD-PEGylated adenovirus vectors into A549 cells and B16BL6 cells. (A) A549 (2×10^4) cells and (B) B16BL6 cells (2×10^4) were transduced with 300, 1000, 3000 or 10000 particles/cell of unmodified Ad, PEG-Ad, RGD-PEG-Ad or Ad-RGD, respectively. Luciferase expression was measured after 24 h. Each point represents the mean ± S.D. (n = 3)

RGD-PEG-Ad retained more than one-tenth of its activity, whereas Ad-RGD lost more than 99% of its activity in the absence of antibody.

RGD-PEG-Ad possessed high gene expression *in vivo*

Unmodified Ad, Ad-RGD, and RGD-PEG-Ad mediated luciferase activity predominantly in the liver after intravenous administration. No significant difference in liver transduction was found between unmodified Ad and RGD-PEG-Ad (Figure 7). Biodistribution of Ad-RGD and RGD-PEG-Ad was similar in lung, spleen, kidney, heart and brain (data not shown).

Discussion

Ads are widely used as vectors for gene therapy experiments. To date, several methods including gutless Ads, which address the decrease in antigenicity [35–37], and fiber mutant Ads [25,38,39], have been developed. In the present study, we initially focused on the modification of Ads by PEG because of its relative ease of development and many other merits such as evasion of neutralizing antibodies. However, as is well known, the conjugation of an Ad with high molecular weight material hinders its interaction with its receptor and subsequently influences the introduction of the virus. Therefore, our aim was to develop novel vectors that exhibit high gene expression while at the same time maintaining the other merits of PEGylated-Ads.

PEGylation of proteins and liposomes has already been widely employed and increased blood stability and mitigation of side effects have been reported [10,11]. PEGylation of the surface of Ads has several advantages. We and other groups have previously demonstrated that modification of an Ad with PEG protects it from neutralizing antibodies [15,16,31]. Likewise, PEGylation has been reported to extend the half-life of Ads in blood

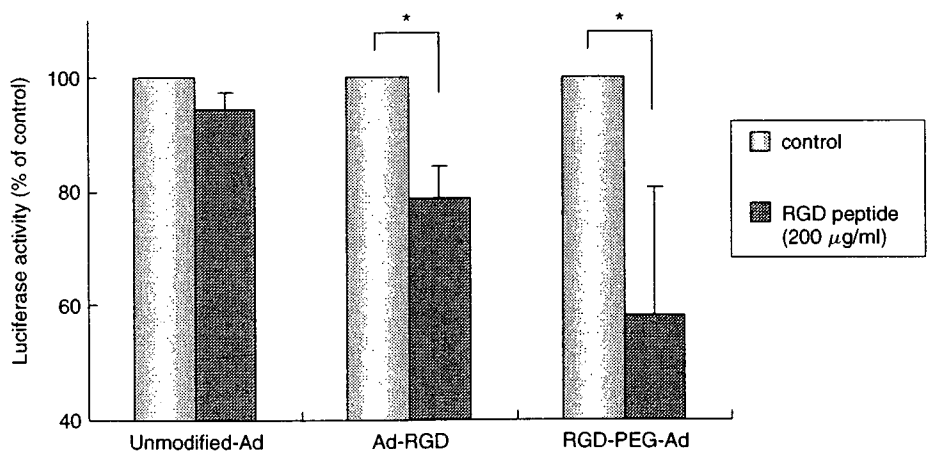

Figure 5. Transduction efficiency of RGD-PEGylated adenovirus vectors in the presence or absence of RGD peptide. B16BL6 cells (2×10^4) were transduced with 3000 particles/cell of unmodified Ad, Ad-RGD or RGD-PEG-Ad in the presence or absence of RGD peptide (200 μg/ml). Luciferase expression was measured after 24 h. Each point represents the mean ± S.D. (n = 3). *$P < 0.05$ (Student's t-test)

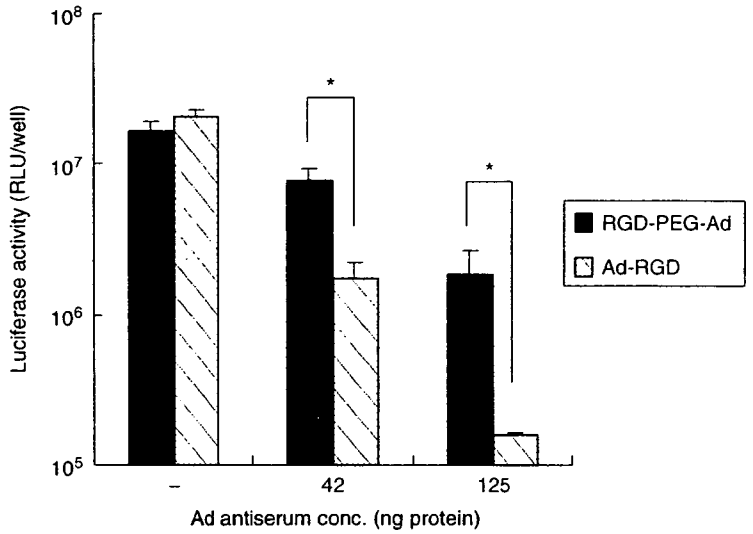

Figure 6. Transduction efficiency of RGD-PEGylated adenovirus vectors in the presence of adenovirus vector antiserum. B16BL6 cells (2×10^4) were transduced with 1000 particles/cell of RGD-PEG-Ad or Ad-RGD in the presence or absence of Ad antiserum. Luciferase expression was measured after 24 h. Each point represents the mean ± S.D. (n = 3). *$P < 0.05$ (Student's t-test)

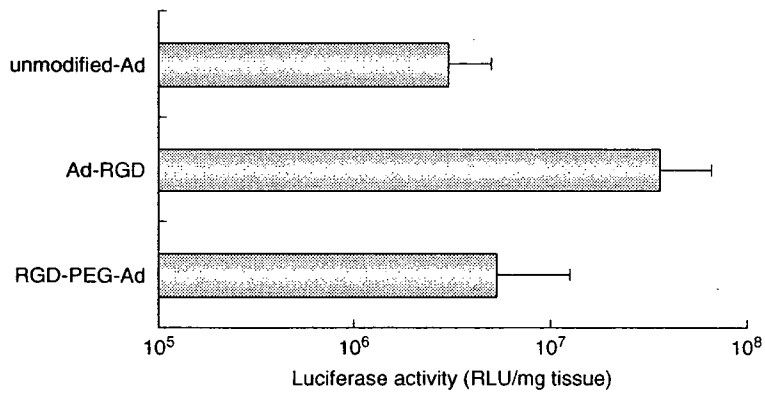

Figure 7. The gene expression in liver induced by RGD-PEG-Ad. 1.5×10^{10} particles of unmodified Ad, Ad-RGD, or RGD-PEG-Ad were injected intravenously. After 2 days, the liver was harvested and homogenized. Luciferase activity was then measured using the kit according to the manufacturer's instructions. Each point represents the mean ± S.D. (n = 4)

[17]. Steric hindrance by PEG chains and masking of the Ad surface electric charge were expected to reduce uptake by Kuppfer cells. In the present study, we established a method that can control the rate of Ad modification, and the results confirmed that PEGylation notably reduced gene expression efficiency in A549 cells. The data also suggest that increased modification with PEG induced lower gene expression (Figure 1).

In a clinical setting, the most serious problem associated with PEG-Ads is the decrease in transduction. We determined that this decrease results from the inhibition of Ad and CAR interaction due to steric hindrance by PEG chains (Figure 2). This suggests that high gene expression can be achieved if PEGylated-Ads can be transduced into cells. Therefore, in the present study, we focused on the RGD motif, which mediates the entrance of Ads into cells following the interaction with integrin [23,24]. We initially constructed RGD-PEG, which contains the RGD peptide at the tip of PEG, and reacted it with Ad to form RGD-PEG-Ad. The data in Table 1 demonstrate that the vector size of RGD-PEG-Ad was 12 nm bigger than that of unmodified Ad, and the same tendency was observed in the case of PEG-Ads. The size of Ads increased to about 10–15 nm at a PEG modification rate of 30–40% (data not shown). We thereby succeeded in developing a novel PEG-Ad, the efficacy of which was not influenced by the combination with PEG.

RGD-PEG-Ad gene expression in A549 cells was significantly higher than that of PEG-Ad, and was equivalent to conventional Ad and Ad-RGD (Figure 4). In CAR-negative B16BL6 cells, RGD-PEG-Ad also showed enhanced gene expression, which was much higher than that of PEG-Ads or conventional Ads. Because CAR is expressed at low levels in certain cells, such as hematopoietic stem cells, peripheral blood cells, differentiated airway epithelium, muscle cells, most mouse-derived cells, and many tumor cells, this novel PEGylated Ad is attractive for gene therapy. In addition,

our RGD-PEG-Ad was very stable under −80 °C storage conditions, despite several cycles of freezing and thawing (data not shown).

We also checked the specificity of RGD-PEG-Ad infection; we measured the gene expression of unmodified Ad, Ad-RGD, and RGD-PEG-Ad in the presence or absence of competitive RGD peptide (Figure 5). Koizumi *et al.* [25] have already reported the specificity of infection of Ad-RGD through integrin. In the present study, RGD-PEG-Ad gene expression was significantly inhibited by RGD peptide, GRGDTP, and, because RGD-PEG-Ad gene expression in CAR-negative, integrin-positive cells was notably enhanced compared to that of PEG-Ad, we suggest that the transduction of RGD-PEG-Ad was integrin-dependent.

Moreover, we determined whether RGD-PEG-Ad improved resistance to neutralizing antibodies (Figure 6). The expression of Ad-RGD genes fell remarkably in the presence of Ad antiserum. However, we demonstrated that RGD-PEG-Ad gene expression was far higher than that of Ad-RGD in the presence of the antiserum. This ability to evade antibodies is essential for clinical applications because nearly 80% of human patients possess anti-Ad antibodies, and re-administration is indispensable in some cases. Therefore, RGD-PEG-Ad minimizes the amount of medication required and reduces side effects.

The method described here is also applicable to other virus vectors and other target molecules. We are currently screening the use of peptides or antibodies as antigens or tissue-specific targeting molecules using the phage display system. These approaches will promote the development of a virus vector that exhibits enhanced safety and applicability.

Acknowledgements

This study was supported in part by the Research on Health Sciences focusing on Drug Innovation from The Japan Health Sciences Foundation; by Grants-in-Aid for Exploratory Research from the Ministry of Education, Culture, Sports, Science and Technology of Japan; and by grants from the Ministry of Health and Welfare in Japan.

References

1. Gao JQ, Tsuda Y, Katayama K, *et al.* Antitumor effect by interleukin-11 receptor alpha-locus chemokine/CCL27, introduced into tumor cells through a recombinant adenovirus vector. *Cancer Res* 2003; **63**: 4420–4425.
2. Crystal RG. Transfer of genes to humans: early lessons and obstacles to success. *Science* 1995; **270**: 404–410.
3. Wilson JM. Adenoviruses as gene-delivery vehicles. *N Engl J Med* 1996; **334**: 1185–1187.
4. Smith TA, Mehaffey MG, Kayda DB, *et al.* Adenovirus mediated expression of therapeutic plasma levels of human factor IX in mice. *Nat Genet* 1993; **5**: 397–402.
5. Wohlfart C. Neutralization of adenoviruses: kinetics, stoichiometry, and mechanisms. *J Virol* 1988; **62**: 2321–2328.
6. Mastrangeli A, Harvey BG, Yao J, *et al.* "Sero-switch" adenovirus-mediated in vivo gene transfer: circumvention of anti-adenovirus humoral immune defenses against repeat adenovirus vector administration by changing the adenovirus serotype. *Hum Gene Ther* 1996; **7**: 79–87.
7. Mizuguchi H, Koizumi N, Hosono T, *et al.* A simplified system for constructing recombinant adenoviral vectors containing heterologous peptides in the HI loop of their fiber knob. *Gene Ther* 2001; **8**: 730–735.
8. Yei S, Mittereder N, Tang K, *et al.* Adenovirus-mediated gene transfer for cystic fibrosis: quantitative evaluation of repeated in vivo vector administration to the lung. *Gene Ther* 1994; **1**: 192–200.
9. Croyle MA, Yu QC, Wilson JM. Development of a rapid method for the PEGylation of adenoviruses with enhanced transduction and improved stability under harsh storage conditions. *Hum Gene Ther* 2000; **11**: 1713–1722.
10. Tsutsumi Y, Tsunoda S, Kamada H, *et al.* Molecular design of hybrid tumour necrosis factor-alpha. II. The molecular size of polyethylene glycol-modified tumour necrosis factor-alpha affects its anti-tumour potency. *Br J Cancer* 1996; **74**: 1090–1095.
11. Yoshioka Y, Tsutsumi Y, Ikemizu S, *et al.* Optimal site-specific PEGylation of mutant TNF-alpha improves its antitumor potency. *Biochem Biophys Res Commun* 2004; **315**: 808–814.
12. Romanczuk H, Galer CE, Zabner J, *et al.* Modification of an adenoviral vector with biologically selected peptides: a novel strategy for gene delivery to cells of choice. *Hum Gene Ther.* 1999; **1**: 2615–2626.
13. Croyle MA, Chirmule N, Zhang Y, *et al.* "Stealth" adenoviruses blunt cell-mediated and humoral immune responses against the virus and allow for significant gene expression upon readministration in the lung. *J Virol* 2001; **75**: 4792–4801.
14. Croyle MA, Chirmule N, Zhang Y, *et al.* PEGylation of E1-deleted adenovirus vectors allows significant gene expression on readministration to liver. *Hum Gene Ther* 2002; **10**: 1887–1900.
15. O'Riordan CR, Lachapelle A, Delgado C, *et al.* PEGylation of adenovirus with retention of infectivity and protection from neutralizing antibody in vitro and in vivo. *Hum Gene Ther* 1999; **10**: 1349–1358.
16. Eto Y, Gao JQ, Sekiguchi F, *et al.* Neutralizing antibody evasion ability of adenovirus vector induced by the bioconjugation of MPEG-SPA. *Biol Pharm Bull* 2004; **27**: 936–938.
17. Alemany R, Suzuki K, Curiel DT. Blood clearance rates of adenovirus type 5 in mice. *J Gen Virol* 2000; **81**: 2605–2609.
18. Lanciotti J, Song A, Doukas J, *et al.* Targeting adenoviral vectors using heterofunctional polyethylene glycol FGF2 conjugates. *Mol Ther.* 2003; **8**: 99–107.
19. Ogawara K, Rots MG, Kok RJ, *et al.* A novel strategy to modify adenovirus tropism and enhance transgene delivery to activated vascular endothelial cells in vitro and in vivo. *Hum Gene Ther* 2004; **15**: 433–443.
20. Bergelson JM, Krithivas A, Celi L, *et al.* The murine CAR homolog is a receptor for coxsackie B viruses and adenoviruses. *J Virol* 1998; **72**: 415–419.
21. Tomko RP, Xu R, Philipson L. HCAR and MCAR: the human and mouse cellular receptors for subgroup C adenoviruses and group B coxsackieviruses. *Proc Natl Acad Sci U S A* 1997; **94**: 3352–3356.
22. Bewley MC, Springer K, Zhang YB, *et al.* Structural analysis of the mechanism of adenovirus binding to its human cellular receptor, CAR. *Science* 1999; **286**: 1579–1583.
23. Wickham TJ, Mathias P, Cheresh DA, Nemerow GR. Integrins alpha v beta 3 and alpha v beta 5 promote adenovirus internalization but not virus attachment. *Cell* 1993; **73**: 309–319.
24. Mathias P, Wickham T, Moore M, Nemerow G. Multiple adenovirus serotypes use alpha v integrins for infection. *J Virol* 1994; **68**: 6811–6814.
25. Koizumi N, Mizuguchi H, Hosono T, *et al.* Efficient gene transfer by fiber-mutant adenoviral vectors containing RGD peptide. *Biochim Biophys Acta* 2001; **1568**: 13–20.
26. Reynolds P, Dmitriev I, Curiel D. Insertion of an RGD motif into the HI loop of adenovirus fiber protein alters the distribution of transgene expression of the systemically administered vector. *Gene Ther* 1999; **6**: 1336–1339.
27. Mizuguchi H, Kay MA. Efficient construction of a recombinant adenovirus vector by an improved in vitro ligation method. *Hum Gene Ther* 1998; **9**: 2577–2583.
28. Maizel JV Jr, White DO, Scharff MD. The polypeptides of adenovirus. I. Evidence for multiple protein components in the

virion and a comparison of types 2, 7A, and 12. *Virology* 1968; **36**: 115–125.
29. Rink H. Solid-phase synthesis of protected peptide fragments using a trialkoxydiphenylmethyl ester resin. *Tetrahedron Lett* 1987; **28**: 3787–3790.
30. Sieber P. Modification of tryptophan residues during acidolysis of 4-methoxy-2,3,6-trimethylbenzenesulfonyl groups. *Tetrahedron Lett* 1987; **28**: 1637–1641.
31. Chillon M, Lee JH, Fasbender A, *et al.* Adenovirus complexed with polyethylene glycol and cationic lipid is shielded from neutralizing antibodies in vitro. *Gene Ther* 1998; **5**: 995–1002.
32. Xu ZL, Mizuguchi H, Ishii-Watabe A, *et al.* Optimization of transcriptional regulatory elements for constructing plasmid vectors. *Gene* 2001; **11**: 149–156.
33. Wu ZZ, Li P, Huang QP, *et al.* Inhibition of adhesion of hepatocellular carcinoma cells to basement membrane components by receptor competition with RGD- or YIGSR-containing synthetic peptides. *Biorheology* 2003; **40**: 489–502.
34. Bronson RA, Fusi F. Evidence that an Arg-Gly-Asp adhesion sequence plays a role in mammalian fertilization. *Biol Reprod* 1990; **43**: 1019–1025.
35. Hardy S, Kitamura M, Harris-Stansil T, *et al.* Construction of adenovirus vectors through Cre-lox recombination. *J Virol* 1997; **71**: 1842–1849.
36. Von Seggern DJ, Chiu CY, Fleck SK, *et al.* A helper-independent adenovirus vector with E1, E3, and fiber deleted: structure and infectivity of fiberless particles. *J Virol* 1999; **73**: 1601–1608.
37. Zou L, Zhou H, Pastore L, Yang K. Prolonged transgene expression mediated by a helper-dependent adenoviral vector (hdAd) in the central nervous system. *Mol Ther* 2000; **2**: 105–113.
38. Belousova N, Krendelchtchikova V, Curiel DT, Krasnykh V. Modulation of adenovirus vector tropism via incorporation of polypeptide ligands into the fiber protein. *J Virol* 2002; **76**: 8621–8631.
39. Nicklin SA, Von Seggern DJ, Work LM, *et al.* Ablating adenovirus type 5 fiber-CAR binding and HI loop insertion of the SIGYPLP peptide generate an endothelial cell-selective adenovirus. *Mol Ther* 2001; **4**: 534–542.

GENE DELIVERY

Available online at www.sciencedirect.com

SCIENCE DIRECT

ELSEVIER

Journal of Controlled Release 105 (2005) 344–353

journal of controlled release

www.elsevier.com/locate/jconrel

Fusogenic liposome delivers encapsulated nanoparticles for cytosolic controlled gene release

Jun Kunisawa[a,1], Takashi Masuda[a,1], Kazufumi Katayama[a], Tomoaki Yoshikawa[a,b], Yasuo Tsutsumi[a,b], Mitsuru Akashi[b,c], Tadanori Mayumi[a], Shinsaku Nakagawa[a,b,*]

[a]*Department of Biopharmaceutics, Graduate School of Pharmaceutical Sciences, Osaka University 1-6 Yamadaoka, Suita, Osaka 565-0871, Japan*

[b]*"Creation of bio-devices and bio-systems with chemical and biological molecules for medical use", CREST, Japan Science and Technology Corporation (JST), Japan*

[c]*Department of Nanostructured and Advanced Materials, Graduate School of Science and Engineering, Kagoshima University, Japan*

Received 8 December 2004; accepted 18 March 2005
Available online 3 June 2005

Abstract

Therapeutic agents based on DNA or RNA oligonucleotides (e.g., antisense DNA oligonucleotide, small interfering RNA) require a regulation of their kinetics in cytoplasm to maintain an optimal concentration during the treatment period. In this respect, delivery of functional nanoparticles containing these drugs into cytoplasm has been thought to have a potential for the cytosolic controlled gene release. In this study, we establish a protocol for the encapsulation of nanoparticles into liposome, which is further fused with ultra violet-inactivated Sendai virus to compose fusogenic liposomes. When nanoparticles were encapsulated in conventional liposomes, endocytosis-mediated uptake of nanoparticles was observed. In contrast, numerous amounts of nanoparticles were delivered into the cytoplasm without any cytotoxicity when the particles were encapsulated in fusogenic liposomes. Additionally, fusogenic liposome showed a high ability to deliver nanoparticles containing DNA oligonucleotides into cytoplasm. These results indicate that this combinatorial nanotechnology using fusogenic liposome and nanoparticle is a valuable system for regulating the intracellular pharmacokinetics of gene-based drugs.

Keywords: Fusogenic liposome; Nanoparticle; Nanotechnology; Drug delivery; Antisense oligonucleotide DNA

1. Introduction

Among recent advances in nanotechnology, one of the most prominent progresses is its application to drug delivery. Numerous drug carriers with nanoscale sizes like a nanoparticle (NP), liposome, dendrimer and nanocrystal have been developed and some of

* Corresponding author. Department of Biopharmaceutics, Graduate School of Pharmaceutical Sciences, Osaka University 1-6 Yamadaoka, Suita, Osaka 565-0871, Japan. Tel./fax: +81 6 6879 8176.
E-mail address: nakagawa@phs.osaka-u.ac.jp (S. Nakagawa).
[1] These authors contributed equally to the work.

0168-3659/$ - see front matter © 2005 Elsevier B.V. All rights reserved.
doi:10.1016/j.jconrel.2005.03.020

them are already in clinical use [1–3]. The major aim of these delivery systems is to regulate "systemic pharmacokinetics" such as drug absorption, distribution (e.g., tissue-specific targeting), metabolism and elimination in vivo [4,5]. However, recent advancements on drug design have proposed that the regulation of "intracellular pharmacokinetics" is also important for drugs targeting intracellular components [6,7].

Novel gene-based therapies using an antisense DNA and small interference RNA (siRNA) represent an enormously promising approach to decrease or modulate an expression of their target molecules [7–11]. Since the main physiological target of these drugs is messenger RNA, it is pivotal to deliver them into cytoplasm. Although there are systems, including ours, that can achieve the delivery of soluble drugs into cytoplasm [12–15], a novel delivery system to introduce NPs containing gene-based drugs into cytoplasm will provide further advantages for the maintenance of the optimal concentration by protecting the genes from hydrolytic and enzymatic degradation.

We previously developed fusogenic liposome (FL) having Sendai virus envelope glycoproteins on the surface and reported that FL could efficiently introduce encapsulated nucleotides and/or proteins into the cytoplasm through its direct fusion to the plasma membrane without cytotoxicity [12,16]. We also demonstrated an application of FL to gene therapy, cancer chemotherapy and vaccine development [17–22]. These progressive results lead us to suppose that FL would also be able to transport NP into the cytoplasm if NP would be encapsulated in FL. In the present study, we determine an optimal protocol to encapsulate a NP into conventional liposome (Lipo) and to fuse them subsequently with Sendai virus to formulate FL. We also present that FL shows a high ability to introduce the encapsulated NPs into cytoplasm, which is applicable to cytosolic controlled gene release.

2. Materials and methods

2.1. Preparation of FL encapsulating NP

Lipo was prepared by a dehydration–rehydration method [23]. Briefly, a lipid mixture, composed of phosphatidylcholine, L-α-dimyristoyl phosphatidic acid, and cholesterol (NOF Corporation, Tokyo, Japan) in a 4:5:1 molar ratio, was suspended in solution containing chloroform, methanol and water (65:25:4) and evaporated to remove chloroform and methanol. To label liposomal membrane with rhodamine, rhodamine-labeled diacylphosphatidyl ethanolamine (Molecular Probes, Eugene, OR) was added to the mixture. The lipid mixture was further frozen in liquid nitrogen and lyophilized overnight. The resulting lipid powder was hydrated with solution containing FITC-labeled NP (Molecular Probes) or oligonucleotide-adsorbed NP (about $0.5–3 \times 10^{11}$ particles/ml). Conventional liposome (Lipo) was prepared from the hydrated mixture by a hand-held extruder with two layers of cellulose acetate membranes (pore size, 800 nm in diameter) (Advantec, Osaka, Japan) and washed with phosphate-buffered saline (PBS).

For preparation of FL, NP encapsulated in Lipo (NP–Lipo) was mixed with UV-inactivated Sendai virus and incubated with vigorous shaking for 2 h at 37 °C. FL was finally purified by stepwise sucrose-density centrifugation (77,000 $\times g$, 2 h, 4 °C) as described previously [16].

2.2. Preparation of poly (vinyl amine) NP

Preparation of poly (vinyl amine) NP was described previously [24]. Briefly, poly (vinyl acetamide) macromer was prepared from monomers by free radical polymerization, in which 2,2′-azobisisobutyronitrile (AIBN) and 2-mercaptoethanol were used as an initiator and a chain transfer agent, respectively, and then *p*-chloromethyl styrene was used to introduce a vinyl benzyl group. Nonionic poly (vinyl acetamide) NP was produced by copolymerization between the macromonomers and styrene after initiation with AIBN. Surface cationized poly (vinyl amine) NP was prepared by hydrolyzing poly (vinyl acetamide) NP in 4 N HCl at 80 °C. The resulting poly (vinyl amine) NP was dialyzed to remove unreacted substances and then was lyophilized.

To prepare oligonucleotide-adsorbed NP, poly (vinyl amine) NP (6×10^{10} particles/ml) was mixed with FITC-labeled phosphorothioate oligo deoxynucleotides (GCCCAAGCTGGCATCCGTCA, 3×10^{15} copies/ml, Geneset, Kyoto, Japan) for 1 h at room temperature.

2.3. Transmission electron microscopy (TEM)

To visually examine liposome structure, Cryo-TEM was employed. Specimens were prepared by depositing a small droplet of liposome suspension on a TEM grid coated with poly-lysine, vitrified by plunging it into liquid ethane, and observed by TEM (TECNAI F20TWIN; Phillips, Mahwah, NJ).

For the analysis of intracellular distribution of NP, LLCMK2 cells cultured on collagen-coated plates were treated with NP–FL for 30 min. After washing three times with PBS, the cells were fixed with 2% glutaraldehyde for 2 h at 4 °C and then post-fixed with 1% osmium tetroxide for 2 h at 4 °C. After dehydration by immersing in serially diluted aqueous ethanol solutions, the specimens were embedded in epoxy resin, sectioned to 80–100 nm thick, stained with uranyl acetate, and examined by TEM.

2.4. Confocal microscopy and flow cytometry

LLCMK2, HeLa, HL-60, HUVEC or DC2.4 cells (kindly gifted from Dr. K. Rock, University of Massachusetts Medical School) (10^5 cells/well) were plated in a 24-well plate and were cultured overnight for subsequent experiments. To measure NP delivery, the cells were treated with NP-alone, NP–Lipo, or NP–FL (300 particles/cell) for 30 min, washed, and observed by confocal microscopy (Bio-Rad, Hercules, CA). Simultaneously, nucleus was stained with 1 mM SYTO64 (Molecular Probes).

The treated cells were also dissociated from plates by treating with 0.25% trypsin and were analyzed by FACScan flow cytometer (Becton Dickinson, Mansfield, MA). To inhibit endocytosis, LLCMK2 cells were treated with 5 μg/ml of cytochalasin B or 0.2 μg/ml of cytochalasin D (Sigma, St Louis, MO). Following 1-h incubation, NP–Lipo (3000 particles/cell) or NP–FL (300 particles/cell) were added and the cells were cultured for 30 min. Uptake efficiency was measured by flow cytometry.

2.5. Cytotoxic assay

To assess the cytotoxicity of NP-alone, NP–Lipo or NP–FL, LLCMK2 cells were treated with the particles (300 particles/cell) for 30 min. Following three times washing with PBS, the cells were split into 96-well plate (5×10^2 cells/well) and cultured for 1, 2, 4, or 6 days. The cell viability was determined by 3-(4,5-dimethylthiazol-2-yl)-2,5-diphenyl tetrazolium bromide (MTT).

3. Results and discussion

3.1. Development and characterization of FL containing NP

We firstly evaluated the encapsulation of NP into Lipo using fluorescein isothiocyanate (FITC)-labeled NP (500 nm in diameter) and rhodamine-labeled Lipo. The different densities of empty Lipo ($d = 1.02$) and NP ($d = 1.12$) allowed us to discriminate them by sucrose-density gradient centrifugation. Fluorescence activity derived from empty Lipo and that from NP were detected in fractions 2–3 and fractions 14–15, respectively (Fig. 1A). We also found intermediate fractions (fractions 8–11) exhibiting both NP-derived FITC and Lipo-derived rhodamine fluorescence, which suggested that these fractions contained NP encapsulated in or attached with Lipo (Fig. 1A). To elucidate whether NP was attached with or encapsulated in Lipo, we performed cryo-transmission electron microscopy (Cryo-TEM). This analysis clarified that NP-alone was detected in fractions 14–15 (Fig. 1B) and that NP in fractions 8–11 was surrounded with lipid membrane, indicating that intermediate fractions contained NP encapsulated in Lipo (Fig. 1C).

NP encapsulated in Lipo (NP–Lipo) was then incubated with ultraviolet-inactivated Sendai virus in order to make NP encapsulated in FL (NP–FL). To evaluate the formulation of NP–FL, we mixed fluorescence labeled NP–Lipo with ultraviolet-inactivated Sendai virus followed by analyzing the fluorescence activity after stepwise sucrose-density gradient centrifugation (10%, 30% and 50%). The gradient centrifugation of the mixture resulted in two distinct peaks (Fig. 1D). Cryo-TEM analysis indicated that fractions 8–9 are successfully identical to NP–FL because lipid membrane in the fractions exhibited a spiked structure of envelope proteins derived from Sendai virus (Fig. 1E and F). This conclusion was further confirmed by their diameter and zeta potential at the surface. The diameter of NP–FL (880 nm) is bigger than that of NP–Lipo (750 nm) and

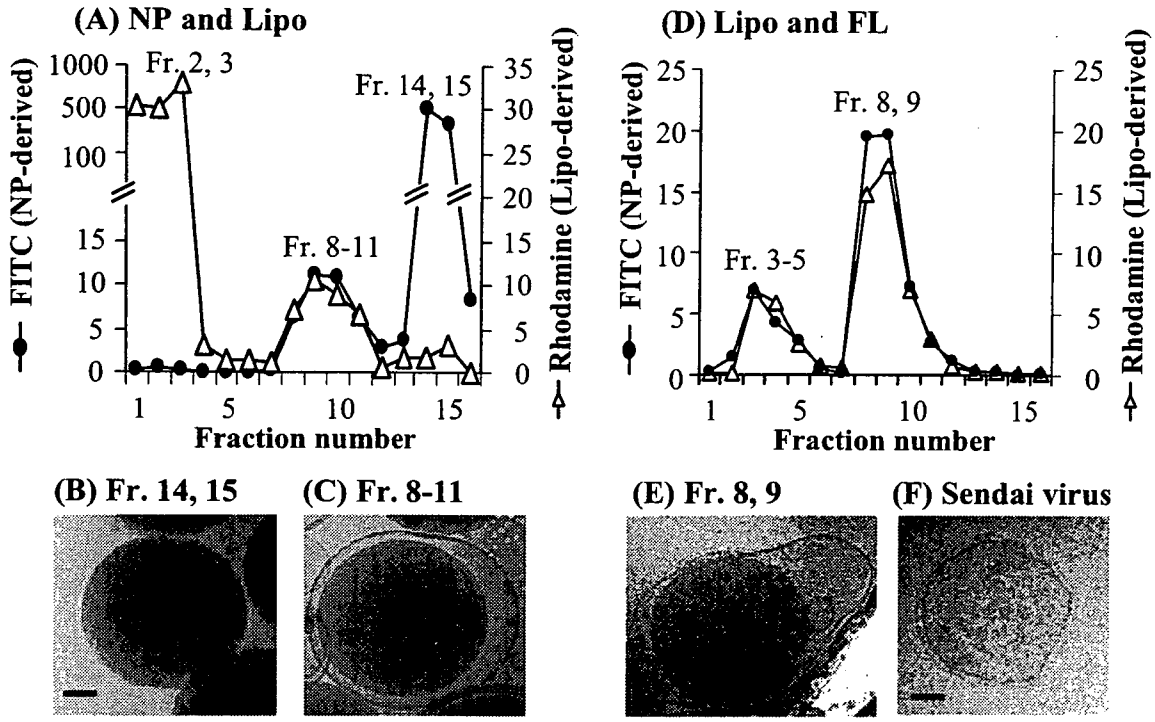

Fig. 1. Characterization of NP–Lipo and NP–FL. (A) FITC-labeled NP was encapsulated in rhodamine-labeled Lipo. After stepwise fractionation through sucrose-density centrifugation (6%, 10% and 30%), fluorescent intensity derived from FITC-NP (closed circle) or rhodamine-Lipo (open triangle) was measured. (B and C) Fractions 14–15 in A (B, NP-alone) or fractions 8–11 in A (C, NP–Lipo) were visualized by Cryo-TEM. Bar corresponds to 100-nm length. (D) NP–FL was prepared by fusing ultraviolet-inactivated Sendai virus with NP–Lipo. The resultant was purified by stepwise sucrose-density centrifugation (10%, 30% and 50%) and fluorescent intensity of each fraction was analyzed as described in A. (E and F) Fractions 8–9 in D (E, NP–FL) or ultraviolet-inactivated Sendai virus (F) were observed by Cryo-TEM. Bar is identical to 100 nm.

of Sendai virus (300 nm). Additionally, surface zeta-potential of fractions 8–9 (−15 mV) was largely different from that of NP–Lipo (−27 mV) because they were affected by the different electronic charge of Sendai virus (−13 mV).

In this study, we used 500 nm NP in diameter. In addition, we also successfully encapsulated 20 nm or 100 nm NP in Lipo as well as FL with equal efficiency (only data using 500 nm NP are shown in this study). Further, we are also capable of regulating the liposomal size by selection of the membrane pore size for the extrusion (the average size of NP–FL used in this study is 880 nm in diameter). Also we can regulate surface electronic characteristics of FL membrane by selecting the lipid composition. These results suggest that the protocol described in this study is a versatile system to encapsulate various sizes of NP into FL with various characteristics.

3.2. Efficient delivery of NP by FL

To examine the feasibility of Lipo and FL as a vehicle to deliver NP, LLCMK2 cells were incubated with FITC-labeled NP encapsulated in either Lipo or FL and were observed by confocal microscopy. In spite of the fact that only a few NPs were observed in the cells incubated with NP-alone or NP–Lipo (Fig. 2A and B), a large number of NPs were detected when the cells were treated with NP–FL (Fig. 2C and D). Simultaneous staining of nucleus with SYTO64 indicated that 500 nm NP was not noticed at the nucleus (Fig. 2C and D). This is a predictable observation because nuclear pore complex can transport a particle within 40 nm in diameter [25].

As a next experiment, flow cytometry analysis was employed to evaluate the efficiency of FL for delivery of the encapsulated NP. Several fluorescent peaks

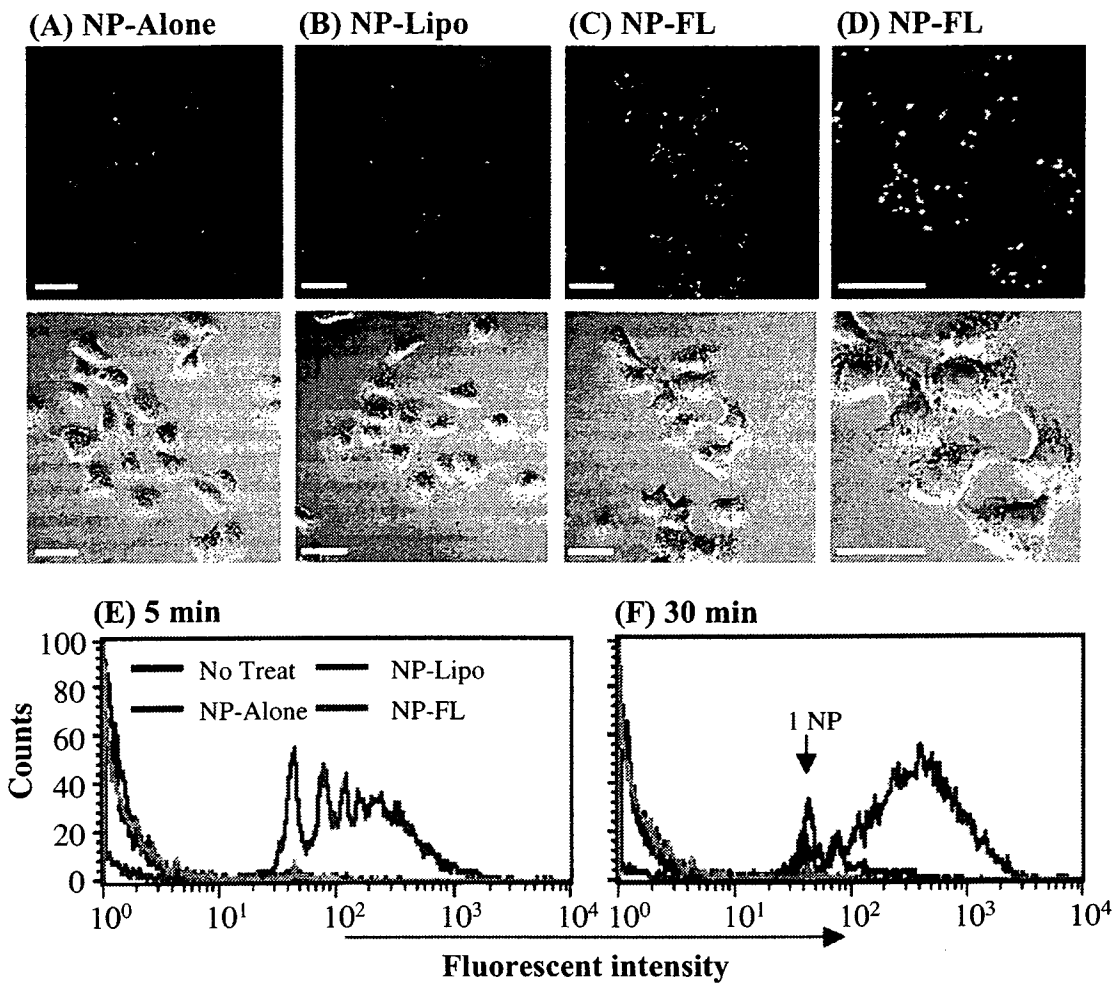

Fig. 2. FL-mediated effective delivery of NP. (A–D) LLCMK2 cells were incubated with FITC-labeled NP without encapsulation (A, NP-alone) or encapsulated in either Lipo (B, NP–Lipo) or FL (C and D, NP–FL) for 30 min. After staining of nucleus with SYTO 64 (red), the cells were observed by confocal microscopy (top). The same specimens were visualized by transmission microscopy (bottom). Bars indicate 50 μm at ×400 (A–C) or ×800 (D) magnification. (E and F) LLCMK2 cells were incubated with NP-alone (green), NP–Lipo (blue), or NP–FL (red) for 5 min (E) or 30 min (F). Fluorescence originated from FITC-labeled NP was measured by a FACScan flow cytometer.

were observed 5 min after the treatment of the cells with NP–FL, whereas fluorescence was barely detectable when the cells were incubated with NP-alone or NP–Lipo (Fig. 2E). This is consistent with our previous result that delivery by FL is mediated by membrane fusion but not by endocytosis, which is faster and more efficient than that of endocytosis-mediated Lipo uptake [16]. Thus, we could detect fluorescence intensity of the cells treated with NP–Lipo after 30 min incubation (Fig. 2F), implying that this uptake might occur through endocytosis. It should be noted that a fluorescence intensity of the cells treated with NP–FL was still much higher than that of the cells incubated with NP-alone or with NP–Lipo after 30-min incubation (Fig. 2F). These results suggested that FL could deliver the encapsulated NPs into the cells in an effective and fast manner.

To show quantitative data for the effective NP delivery, the number of NPs incorporated into a cell after 30-min incubation was calculated by the mean fluorescence intensity of 40 per NP in a cell (arrow, Fig. 2F). Consistent with the results of confocal

Table 1
The number of NPs incorporated in 1 cell was calculated by the result that cells containing 1 NP presented 40 of mean fluorescence intensity after 30 min incubation as described in Fig. 2F

Number	NP-alone	NP–Lipo	NP–FL
0	97.8 ± 0.67	85.8 ± 0.92	5.8 ± 0.38
1–5	2.1 ± 0.06	13.7 ± 0.79	29.9 ± 2.76
6–10	0.1 ± 0.01	0.5 ± 0.13	31.2 ± 1.19
11–25	Undetectable	0.1 ± 0.03	28.9 ± 2.01
26–more	Undetectable	Undetectable	5.3 ± 1.58

Results are expressed as the means ± SE from three independent experiments.

microscopy, NPs were not detected in most cells (97.8%) incubated with NP-alone (Table 1). Similarly, only 1–5 NPs were observed in about 15% of cells incubated with NP–Lipo (Table 1). Conversely, about 95% of cells incubated with NP–FL had detectable NP, with approximately ten NPs per cell on average. Furthermore, about 5% cells contained more than 26 NPs with strong fluorescence intensity (Table 1 and Fig. 2F). These results further emphasize the effectiveness of FL for NP delivery into the cells.

We next investigated the FL-mediated NP delivery into several cell lines to address the specificity. Similar efficiency was determined when NP–FL was incubated with human-derived adherent (HeLa), non-adherent (HL60), and primary culture (HUVEC) cells, while these cells could not take NP-alone or NP–Lipo effectively (Fig. 3A–C). However, murine dendritic cell lines (DC2.4) showed slightly higher uptake activity for NP-alone or NP–Lipo (Fig. 3D). This is due to a high endo-phagocytosis ability of dendritic cell that is well known as an antigen sampling and presenting cells [26]. It should be noted

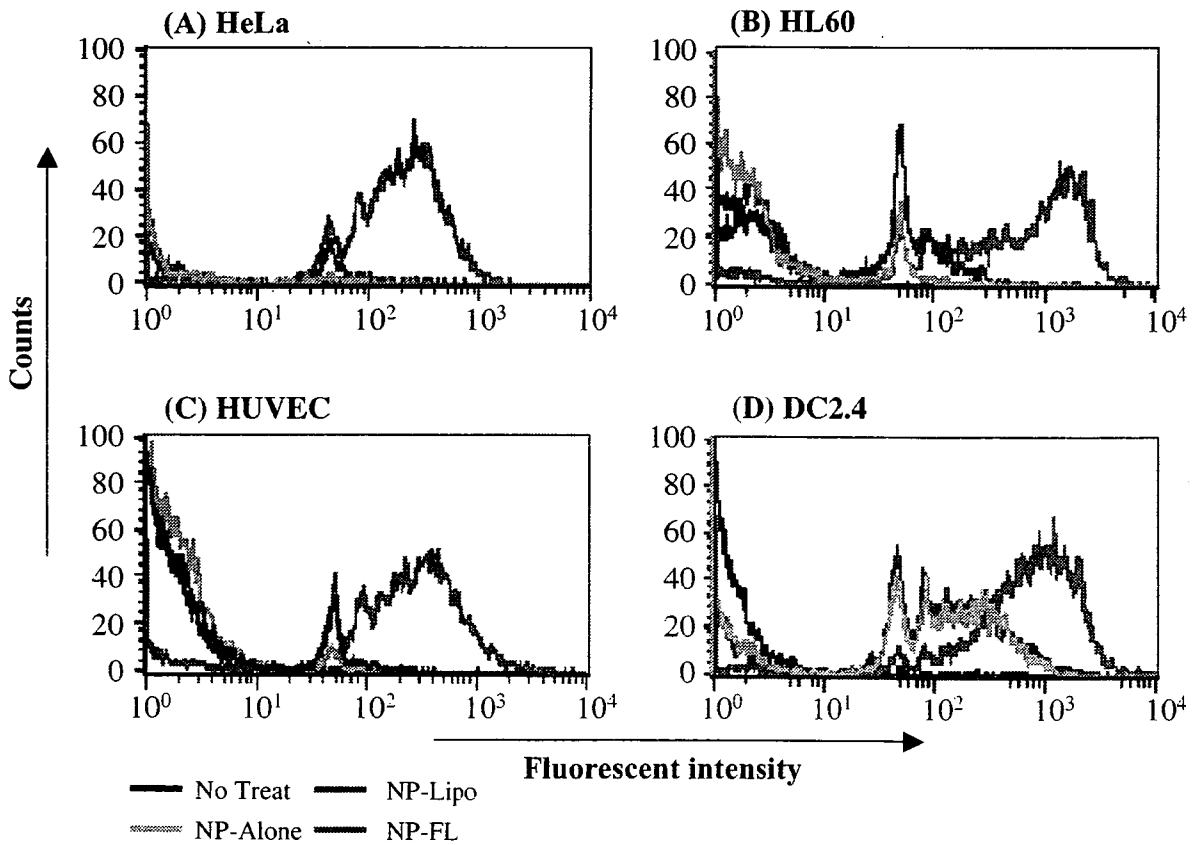

Fig. 3. FL effectively delivers the encapsulated NPs into various kinds of cells. HeLa cells (A), HL60 cells (B), HUVEC (C), or DC2.4 cells (D) were treated with none (black), NP-alone (green), NP–Lipo (blue), or NP–FL (red) for 30 min. Fluorescent intensity in the cell derived from FITC-labeled NP was measured by a FACScan flow cytometer.

again that the number of NPs delivered by FL is still much higher than that of Lipo and the efficiency was not altered in the cells showing high endocytosis activity (Fig. 3D). This observation convinced us that FL-mediated high efficient NP delivery was independent on endocytosis activity. In our previous study, the delivery to a wide variety of cells by FL was also determined and seemed to depend on indiscriminative fusion activity of Sendai virus [27].

3.3. Endocytosis-independent NP delivery into cytoplasm by FL

As mentioned above, FL can efficiently deliver the encapsulated contents to the cytoplasm through its direct fusion with the plasma membrane [16]. Thus, we next tried to test whether NP delivery by FL was also mediated through membrane fusion, rather than through endocytosis. To address this, cells were treated with an endocytosis inhibitor, cytochalasin B or cytochalasin D, followed by the addition of NP–FL or NP–Lipo. While cytochalasin B treatment resulted in a marked reduction of NP–Lipo uptake, no inhibition of NP uptake was observed when cells were incubated with NP–FL (Fig. 4A). Similar results were obtained when cells were treated with the other inhibitors, cytochalasin D (Fig. 4A), 2,4-dinitrophenol, nocodazole or colchicine (data not shown). These results indicated that FL could deliver the encapsulated NPs into the cytoplasm by membrane fusion, rather than by endocytosis. Based on these data, we supposed that NPs delivered by FL was located in cytoplasm, not in endosome. To prove this speculation, TEM analysis was performed to show visually the distribution of NP introduced by FL. The histological analysis showed that NPs existed in the cytoplasm, not in the endosome, of cells treated with NP–FL (Fig. 4B and C).

Most of drug-delivery vehicles, including conventional liposome, enter into cells via endocytosis and then are delivered to lysosomes, where they as well as their contents are degraded [28,29]. Thus, drugs delivered by NP-alone or NP–Lipo are likely degraded in lysosome even if these vehicles are taken up. In contrast, NP–FL can deliver NP efficiently to the cytoplasm not via endocytosis (Figs. 2–4, Table 1). These findings indicated that FL had a benefit not only to deliver the numerous numbers of NP but also to deliver the contents into cytoplasm without their

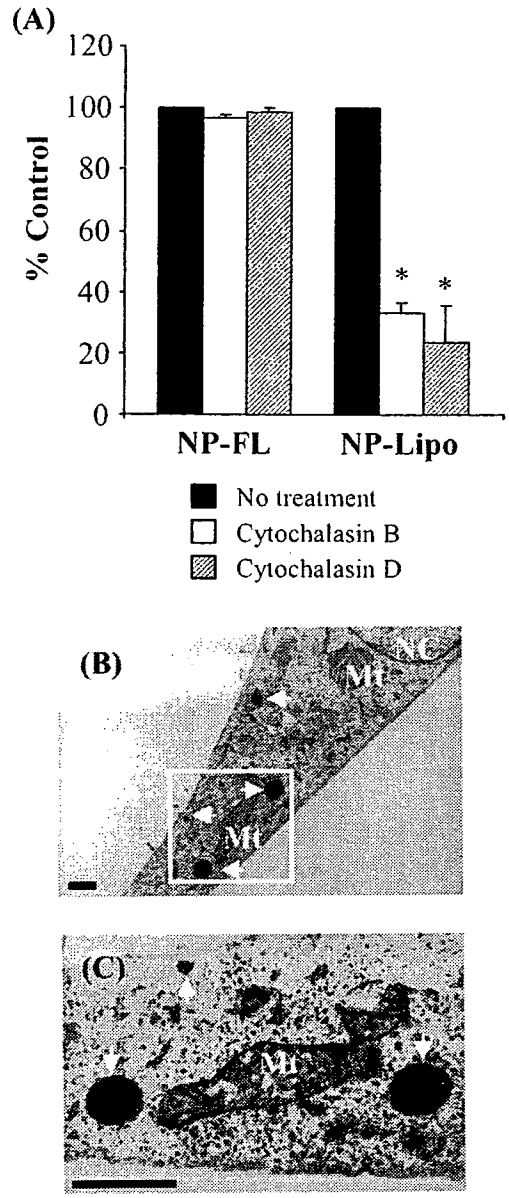

Fig. 4. Endocytosis-independent NP delivery into cytoplasm by FL. (A) LLCMK2 cells were not pre-treated (solid) and pre-treated with 5 μg/ml cytochalasin B (open) or 0.2 μg/ml cytochalasin D (slashed) for 1 h and incubated with NP–FL or NP–Lipo for additional 30 min. Then, the number of FITC-NP positive cells was analyzed by FACScan flow cytometry. Error bars indicate the means ± SE of three independent experiments. (B) LLCMK2 cells were cultured with NP–FL for 30 min and observed by Cryo-TEM. Mitochondrion and nucleus are marked with 'Mt' and 'NC', respectively. Arrowheads indicate NPs. Bars are 1 μm at ×7000 (B) or ×20,000 (D) magnification.

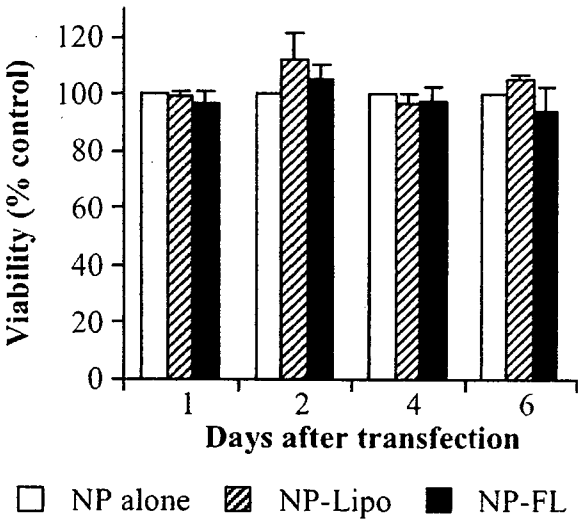

Fig. 5. Toxicity of NP-alone, NP–Lipo, or NP–FL. The NP-alone (open), NP–Lipo (hatched), and NP–FL (closed) were incubated with LLCMK2 cells for 30 min. Following washing with PBS, the cells were cultured for 1, 2, 4, and 6 days. MTT assay was performed to determine the cell viability.

degradation in endosome/lysosome pathway. Furthermore, MTT assay revealed that NP–FL did not show any cytotoxicity against target cells for at least one week after the transfection (Fig. 5).

In this study, we used non-degradable NPs as a model NP. The experimental restriction in cell culture made it difficult to determine the fate of the NPs after the long culture. One possible hypothetical pathway is that NP is excluded to extracellular compartments by exocytosis pathway and/or cell death. Since the non-degradable NPs are difficult to be applied to in vivo use, our current study to expand this technology to biodegradable NPs (e.g., poly lactic acid NPs) is ongoing. Nevertheless, this study allows us to propose that the FL technology has the following advantages over other vehicles: efficient delivery of its contents to the cytoplasm of a wide range of target cells, lack of cytotoxicity, and ease of encapsulation of various NPs.

3.4. Controlled release of DNA oligonucleotides from NP in cytoplasm

To show a potential application of NP–FL system for gene delivery, we examined delivery of DNA oligonucleotides by NP–FL. FITC-labeled phosphorothioate oligonucleotides were immobilized on poly (vinyl amine) NP and were encapsulated into FL. Similar to the above observations (Figs. 2 and 3), flow cytometry analysis demonstrated that delivery efficiency of NP–FL was superior to that of NP–Lipo or NP-alone (Fig. 6). Inhibitor experiments also convinced us that the FL-mediated NP delivery depended on fusion activity of FL (data not shown).

We used in this study single type of NP for gene delivery experiment. Progresses on particle technology in the last decade allow us to select NPs exhibiting a different drug release profile by their characteristics (e.g., surface electron characteristics, hydrophile–lipophile balance) [30–32]. Since FL can encapsulate and deliver various kinds of NP into cells, NPs with different drug release profiles can be introduced into a cell, which may present the "timing drug release". This system is now under investigation. In addition to the modification of encapsulated NPs, our present effort is aimed to demonstrate the feasibility of FL-mediated NP delivery for gene therapy using bioactive DNA and/or RNA oligonucleotides (e.g., RNA interference).

Some groups have already demonstrated the cytosolic particle delivery. Panyam et al. reported that poly (DL-lactide-co-glycolide) NPs were delivered into cytosol by endo-lysosomal escape mechanism [33]. Although they showed an application of that

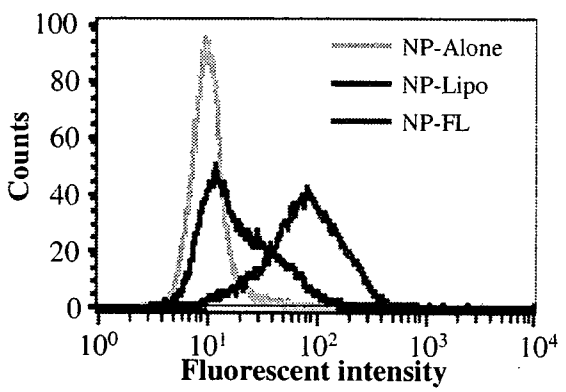

Fig. 6. Efficient delivery of NP containing DNA oligonucleotides into cytoplasm by FL. LLCMK2 cells were cultured with oligonucleotide-immobilized NPs without encapsulation (green) or encapsulated in either Lipo (blue) or FL (red) for 30 min. Fluorescent intensity of the cells were analyzed by a FACScan flow cytometer.

system to intracellular drug release (e.g., dexamethasone and plasmid) from the NPs, we can assert that our NP delivery system is more efficient than their system because the efficacy of FL-mediated NP delivery was much higher than that of endocytosis-mediated uptake even in dendritic cells having a high ability to do endocytosis or phagocytosis (Fig. 3D). In the other approach, HIV-derived TAT peptide was employed for cytoplasmic NP delivery. It was demonstrated that TAT peptide-attached liposome was delivered into cells [34]. Additionally, the group also illustrated the application of TAT-attached liposome to DNA delivery in vitro and in vivo [35]. This is an interesting approach, but they have not unfortunately been succeeded in sustained drug release because the liposome was degraded quickly (within 24 h). Thus, we emphasize that this study demonstrated for the first time that NP is delivered by FL into cytoplasm for the possible application to sustained gene release.

4. Conclusion

In conclusion, we establish a protocol to encapsulate NP into FL and demonstrate that FL is an effective delivery vehicle to introduce the encapsulated NP into cytoplasm. We propose here that the combinatorial nanotechnology, NP–FL, will provide an opportunity for the kinetics regulation of genetic drugs in the cytoplasm.

Acknowledgments

We are grateful to Mr. M. Mori and Mr. K. Sakaguchi at NOF Corporation for supplying us with lipid mixture. We also acknowledge Mr. T. Watanabe at FEI Company for his technical assistance on an electron microscopy study and Dr. Susan Schwab for careful reading of the manuscript. This study was supported in part by Core Research for the Evolutional Science and Technology Program, Japan Science and Technology Corp. and by Grant-in-Aid for Scientific Research (B) from the Ministry of Education, Culture, Sports, Science, and Technology of Japan. J. Kunisawa is a research fellow of the Japan Society for the Promotion of Science.

References

[1] D.A. LaVan, D.M. Lynn, R. Langer, Moving smaller in drug discovery and delivery, Nat. Rev. Drug Discov. 1 (1) (2002) 77–84.
[2] R. Duncan, The dawning era of polymer therapeutics, Nat. Rev. Drug Discov. 2 (5) (2003) 347–360.
[3] H. Otsuka, Y. Nagasaki, K. Kataoka, PEGylated nanoparticles for biological and pharmaceutical applications, Adv. Drug Deliv. Rev. 55 (3) (2003) 403–419.
[4] R.M. Schek, S.J. Hollister, P.H. Krebsbach, Delivery and protection of adenoviruses using biocompatible hydrogels for localized gene therapy, Molec. Ther. 9 (1) (2004) 130–138.
[5] M.E. Akerman, W.C. Chan, P. Laakkonen, S.N. Bhatia, E. Ruoslahti, Nanocrystal targeting in vivo, Proc. Natl. Acad. Sci. U. S. A. 99 (20) (2002) 12617–12621.
[6] J. Alper, Drug delivery. Breaching the membrane, Science 296 (5569) (2002) 838–839.
[7] J.B. Opalinska, A.M. Gewirtz, Nucleic-acid therapeutics: basic principles and recent applications, Nat. Rev. Drug Discov. 1 (7) (2002) 503–514.
[8] Y.S. Cho-Chung, Antisense DNAs as targeted genetic medicine to treat cancer, Arch. Pharm. Res. 26 (3) (2003) 183–191.
[9] T. Suwanmanee, H. Sierakowska, S. Fucharoen, R. Kole, Repair of a splicing defect in erythroid cells from patients with beta-thalassemia/HbE disorder, Molec. Ther. 6 (6) (2002) 718–726.
[10] N.R. Wall, Y. Shi, Small RNA: can RNA interference be exploited for therapy? Lancet 362 (9393) (2003) 1401–1403.
[11] E. Song, S.K. Lee, J. Wang, N. Ince, N. Ouyang, J. Min, J. Chen, P. Shankar, J. Lieberman, RNA interference targeting Fas protects mice from fulminant hepatitis, Nat. Med. 9 (3) (2003) 347–351.
[12] J. Kunisawa, S. Nakagawa, T. Mayumi, Pharmacotherapy by intracellular delivery of drugs using fusogenic liposomes: application to vaccine development, Adv. Drug Deliv. Rev. 52 (3) (2001) 177–186.
[13] N. Murthy, M. Xu, S. Schuck, J. Kunisawa, N. Shastri, J.M. Frechet, A macromolecular delivery vehicle for protein-based vaccines: acid-degradable protein-loaded microgels, Proc. Natl. Acad. Sci. U. S. A. 100 (9) (2003) 4995–5000.
[14] M.C. Morris, J. Depollier, J. Mery, F. Heitz, G. Divita, A peptide carrier for the delivery of biologically active proteins into mammalian cells, Nat. Biotechnol. 19 (12) (2001) 1173–1176.
[15] E. Mathew, G.E. Hardee, C.F. Bennett, K.D. Lee, Cytosolic delivery of antisense oligonucleotides by listeriolysin O-containing liposomes, Gene Ther. 10 (13) (2003) 1105–1115.
[16] H. Mizuguchi, T. Nakagawa, M. Nakanishi, S. Imazu, S. Nakagawa, T. Mayumi, Efficient gene transfer into mammalian cells using fusogenic liposome, Biochem. Biophys. Res. Commun. 218 (1) (1996) 402–407.
[17] H. Mizuguchi, T. Nakagawa, S. Toyosawa, M. Nakanishi, S. Imazu, T. Nakanishi, Y. Tsutsumi, S. Nakagawa, T. Hayakawa, N. Ijuhin, T. Mayumi, Tumor necrosis factor alpha-mediated tumor regression by the in vivo transfer of genes into the artery that leads to tumors, Cancer Res. 58 (24) (1998) 5725–5730.

[18] H. Mizuguchi, M. Nakanishi, T. Nakanishi, T. Nakagawa, S. Nakagawa, T. Mayumi, Application of fusogenic liposomes containing fragment A of diphtheria toxin to cancer therapy, Br. J. Cancer 73 (4) (1996) 472–476.

[19] T. Nakanishi, A. Hayashi, J. Kunisawa, Y. Tsutsumi, K. Tanaka, Y. Yashiro-Ohtani, M. Nakanishi, H. Fujiwara, T. Hamaoka, T. Mayumi, Fusogenic liposomes efficiently deliver exogenous antigen through the cytoplasm into the MHC class I processing pathway, Eur. J. Immunol. 30 (6) (2000) 1740–1747.

[20] A. Hayashi, T. Nakanishi, J. Kunisawa, M. Kondoh, S. Imazu, Y. Tsutsumi, K. Tanaka, H. Fujiwara, T. Hamaoka, T. Mayumi, A novel vaccine delivery system using immunopotentiating fusogenic liposomes, Biochem. Biophys. Res. Commun. 261 (3) (1999) 824–828.

[21] J. Kunisawa, T. Nakanishi, I. Takahashi, A. Okudaira, Y. Tsutsumi, K. Katayama, S. Nakagawa, H. Kiyono, T. Mayumi, Sendai virus fusion protein mediates simultaneous induction of MHC class I/II-dependent mucosal and systemic immune responses via the nasopharyngeal-associated lymphoreticular tissue immune system, J. Immunol. 167 (3) (2001) 1406–1412.

[22] G. Sakaue, T. Hiroi, Y. Nakagawa, K. Someya, K. Iwatani, Y. Sawa, H. Takahashi, M. Honda, J. Kunisawa, H. Kiyono, HIV mucosal vaccine: nasal immunization with gp160-encapsulated hemagglutinating virus of Japan-liposome induces antigen-specific CTLs and neutralizing antibody responses, J. Immunol. 170 (1) (2003) 495–502.

[23] K. Yachi, H. Harashima, H. Kikuchi, R. Sudo, H. Yamauchi, K. Ebihara, H. Matsuo, K. Funato, H. Kiwada, Biopharmaceutical evaluation of the liposomes prepared by rehydration of freeze-dried empty liposomes (FDELs) with an aqueous solution of a drug, Biopharm. Drug Dispos. 17 (7) (1996) 589–605.

[24] S. Sakuma, N. Suzuki, R. Sudo, K. Hiwatari, A. Kishida, M. Akashi, Optimized chemical structure of nanoparticles as carriers for oral delivery of salmon calcitonin, Int. J. Pharm. 239 (1–2) (2002) 185–195.

[25] N. Pante, M. Kann, Nuclear pore complex is able to transport macromolecules with diameters of about 39 nm, Mol. Biol. Cell 13 (2) (2002) 425–434.

[26] Z. Shen, G. Reznikoff, G. Dranoff, K.L. Rock, Cloned dendritic cells can present exogenous antigens on both MHC class I and class II molecules, J. Immunol. 158 (6) (1997) 2723–2730.

[27] M. Nakanishi, H. Mizuguchia, K. Ashihara, T. Senda, T. Akuta, J. Okabe, E. Nagoshi, A. Masago, A. Eguchi, Y. Suzuki, H. Inokuchi, A. Watabe, S. Ueda, T. Hayakawa, T. Mayumi, Gene transfer vectors based on Sendai virus, J. Control. Release 54 (1) (1998) 61–68.

[28] D.P. Howell, R.J. Krieser, A. Eastman, M.A. Barry, Deoxyribonuclease II is a lysosomal barrier to transfection, Molec. Ther. 8 (6) (2003) 957–963.

[29] C.M. Wiethoff, C.R. Middaugh, Barriers to nonviral gene delivery, J. Pharm. Sci. 92 (2) (2003) 203–217.

[30] Y. Ogawa, Injectable microcapsules prepared with biodegradable poly(alpha-hydroxy) acids for prolonged release of drugs, J. Biomater. Sci., Polym. Ed. 8 (5) (1997) 391–409.

[31] S.B. La, T. Okano, K. Kataoka, Preparation and characterization of the micelle-forming polymeric drug indomethacin-incorporated poly(ethylene oxide)-poly(beta-benzyl L-aspartate) block copolymer micelles, J. Pharm. Sci. 85 (1) (1996) 85–90.

[32] J. Kunisawa, A. Okudaira, Y. Tsutusmi, I. Takahashi, T. Nakanishi, H. Kiyono, T. Mayumi, Characterization of mucoadhesive microspheres for the induction of mucosal and systemic immune responses, Vaccine 19 (4–5) (2000) 589–594.

[33] J. Panyam, W.Z. Zhou, S. Prabha, S.K. Sahoo, V. Labhasetwar, Rapid endo-lysosomal escape of poly(DL-lactide-co-glycolide) nanoparticles: implications for drug and gene delivery, FASEB J. 16 (10) (2002) 1217–1226.

[34] V.P. Torchilin, R. Rammohan, V. Weissig, T.S. Levchenko, TAT peptide on the surface of liposomes affords their efficient intracellular delivery even at low temperature and in the presence of metabolic inhibitors, Proc. Natl. Acad. Sci. U. S. A. 98 (15) (2001) 8786–8791.

[35] V.P. Torchilin, T.S. Levchenko, R. Rammohan, N. Volodina, B. Papahadjopoulos-Sternberg, G.G. D'Souza, Cell transfection in vitro and in vivo with nontoxic TAT peptide–liposome–DNA complexes, Proc. Natl. Acad. Sci. U. S. A. 100 (4) (2003) 1972–1977.

Anti-tumor Responses Induced by Chemokine CCL19 Transfected into an Ovarian Carcinoma Model *via* Fiber-Mutant Adenovirus Vector

Jian-Qing GAO,[a,b] Toshiki SUGITA,[a] Naoko KANAGAWA,[a] Keisuke IIDA,[a] Naoki OKADA,[c] Hiroyuki MIZUGUCHI,[a,d] Takashi NAKAYAMA,[e] Takao HAYAKAWA,[f] Osamu YOSHIE,[e] Yasuo TSUTSUMI,[a,d] Tadanori MAYUMI,[a] and Shinsaku NAKAGAWA*,[a]

[a] *Department of Biopharmaceutics, Graduate School of Pharmaceutical Sciences, Osaka University; 1–6 Yamadaoka, Suita, Osaka 565–0871, Japan:* [b] *Department of Pharmaceutics, College of Pharmaceutical Sciences, Zhejiang University; 353 Yan-an Road, Hangzhou, Zhejiang 310031, P. R. China:* [c] *Department of Biopharmaceutics, Kyoto Pharmaceutical University; 5 Nakauchi-cho, Misasagi, Yamashina-ku, Kyoto 607–8414, Japan:* [d] *National Institute of Biomedical Innovation; 7–6–8 Saito-Asagi, Ibaraki, Osaka 567–0085, Japan:* [e] *Department of Microbiology, Kinki University School of Medicine; Osaka-Sayama, Osaka 589–8511, Japan: and* [f] *National Institute of Health Sciences; 1–18–1 Kamiyoga, Setagaya-ku, Tokyo 158–8501, Japan.*

Received March 2, 2005; accepted March 18, 2005; published online March 23, 2005

Considerable attention has recently been paid to the application of chemokines to cancer immunotherapy because of their chemotactic affinity for a variety of immune cells and because several chemokines are strongly angiostatic. In the present study, the recombinant adenovirus vectors encoding chemokine CCL19 or XCL1 in an E1 cassette (AdRGD-mCCL19 and AdRGD-mXCL1) were developed. The constructed fiber-mutant adenovirus vector, which contained the integrin-targeting Arg-Gly-Asp (RGD) sequence in the fiber knob, notably enhanced the transfection efficiency to OV-HM ovarian carcinoma cells compared to that induced by conventional adenovirus vector. The results of an *in vitro* chemotaxis assay for chemokine-encoding vector demonstrated that both AdRGD-mCCL19 and AdRGD-mXCL1 could induce the migration of cells expressing specific chemokine receptors. Of the two chemokine-encoding vectors evaluated *in vivo*, AdRGD-mCCL19 showed significant tumor-suppressive activity in B6C3F1 mice *via* transduction into OV-HM cells, whereas XCL1 did not exhibit any notable anti-tumor effects, suggesting that CCL19 may be a candidate for cancer immunotherapy.

Key words chemokine; CCL19; XCL1; recombinant adenovirus vector; anti-tumor effect; OV-HM cell

Chemokines attract a variety of immune cells and function at inflammatory disease sites as well as lymphoid tissue.[1,2] Considering the eradication of tumor cells as a consequence of interaction with immune cells that have migrated and accumulated in tumor tissue, the usefulness of chemokines for cancer immunotherapy has received considerable attention.[3] By now, more than 40 chemokines have been well characterized, but only a few have been identified as candidates for cancer therapy either independently or with an adjuvant. Tumor-suppressive activity of several chemokines has been observed after transduction into a variety of experimental tumors.[4—7] Tumor cells that were transduced with the CC chemokine gene, CCL3, had reduced tumorgenicity and significantly increased infiltration of macrophages and neutrophils.[8] Another CC chemokine, CCL22, was also strongly chemoattractive to dendritic cells, NK cells and T cells, which resulted in tumor regression in a murine lung carcinoma model due to its efficient induction of anti-tumor immunity.[9] In the present study, we constructed the recombinant viral vector for efficient gene transfection and evaluated the CC family chemokine, EBI1-ligand chemokine (CCL19), and C family chemokine, lymphotactin (XCL1). CCL19 has been shown to chemoattract $CD4^+$, $CD8^+$ T cells and dendritic cells,[11,12] whereas XCL1 is chemotactic for T cells and NK cells but not for monocytes, neutrophils or dendritic cells.[13,14] We anticipated that if tumor cells could be genetically modified by an efficient gene transfer system *in vitro* to produce chemokines *in vivo*, the chemokines could induce accumulation of immune cells in the tumor. The *in vivo* interaction of T cells with the tumor cells should induce anti-tumor immunity, resulting in suppression of tumor growth.

In the present study, we used the adenovirus vector, which exhibits very high gene transduction efficiency.[15] Because a variety of tumor cells contain few Coxsackie adenovirus receptors (CAR),[16] we used a recombinant adenovirus vector with a fiber mutation containing the Arg-Gly-Asp (RGD) sequence in the fiber knob. This fiber-mutant vector possesses higher transduction and anti-tumor activities compared to conventional adenovirus vectors when used in cytokine-gene therapy against melanoma.[17,18] In the present study, ovarian carcinoma OV-HM cells were transfected with a chemokine-encoding recombinant vector, AdRGD-mCCL19 or AdRGD-mXCL1, and both the *in vitro* chemotactive activity and the *in vivo* tumor-suppressive response were investigated.

MATERIALS AND METHODS

Cell Lines and Animals OV-HM ovarian carcinoma cell line[19] were kindly provided by Dr. Hiromi Fujiwara (School of Medicine, Osaka University, Japan) and were maintained in RPMI 1640 supplemented with 10% heat-inactivated FBS. A549 human lung carcinoma cells and human embryonic kidney (HEK) 293 cells were cultured in DMEM supplemented with 10% FBS. Murine pre-B lymphoma L1.2 cells and their stable transfectants, L1.2/mCCR7 and L1.2/mXCR cells, which expressing specific receptor for CCL19 and XCL1, respectively, were maintained in RPMI 1640 supplemented with 10% heat-inactivated FBS and 2-ME (50 μM, Life Technologies). All the cell lines were cultured at 37 °C in a humidified atmosphere with 5% CO_2. Female B6C3F1 mice were purchased from SLC Inc. (Hamamatsu, Japan) and used at 6—8 weeks of age. All of the experimental pro-

* To whom correspondence should be addressed. e-mail: nakagawa@phs.osaka-u.ac.jp

cedures were in accordance with the Osaka University guidelines for the welfare of animals in experimental neoplasia.

Construction of Adenovirus Vectors The replication-deficient adenovirus vectors containing a fiber mutation, which were used in this study, were developed based on the adenovirus type 5 backbone with deletions of the E1 and E3 regions.[20] The RGD sequence was inserted into the HI loop of the fiber knob using a two-step method developed by Mizuguchi *et al.*[21] Murine chemokine genes derived from pT7T3D-Pac-mCCL19 and pExCell-mCXL1 were used as sources of cDNA. Recombinant adenovirus vectors with the RGD fiber mutation, AdRGD-mCCL19 and AdRGD-mXCL1, carrying the chemokine cDNA under the control of the cytomegalovirus (CMV) promoter, were constructed by an improved *in vitro* ligation method described previously.[20,22] The luciferase expressing adenovirus vectors with the RGD fiber mutation (AdRGD-luc), serving as a negative control, is identical to the AdRGD-mCCL19 and AdRGD-mXCL1 vectors and contains the luciferase gene in the expression cassette (Fig. 1). Conventional adenovirus vector expressing lusiferase (Ad-Luc) was also developed by Mizuguchi *et al.*[22] The adenovirus vectors were propagated in 293 cells and purified by cesium chloride gradient ultracentrifugation. Virus particle (VP) was accomplished spectrophotometrically.[23] The titer (tissue culture infectious $dose_{50}$; $TCID_{50}$) was determined by plaque-forming assay using 293 cells.[24,25]

Gene Expression by AdRGD-Luc or Conventional Ad-Luc in OV-HM Ovarian Carcinoma Cells 2×10^3 of OV-HM cells in a 96-well plate were treated with Ad-Luc or AdRGD-Luc at 1250, 2500, 5000, and 10000 viral particles/cell for 1.5 h, respectively. Cells were washed with PBS and cultured for an additional 48 h. Subsequently, the cells were washed, collected, and their luciferase activity was measured using the Luciferase Assay System (Promega, U.S.A.) and Microlumat Plus LB96 (Perkin Elmer, U.S.A.) after the cells were lysed with the Luciferase Cell Culture Lysis (Promega, U.S.A.) according to the manufacturer's instruction.

***In Vitro* Chemotaxis Assay** The AdRGD-Luc and indicated AdRGD-chemokine were tranfected into A549 cells for 2 h at a multiplicity of infection (MOI) of 50, and the cells were washed twice with PBS and cultured in media containing 10% FBS. The cells were subsequently washed after 24 h cultivation, and incubated with an assay medium (phenol red-free RPMI 1640 containing 0.5% bovine serum albumin and 20 μM HEPES, pH 7.4) for another 24 h. The resulting conditioned medium was collected, and its chemoattractant activity was measured by an *in vitro* chemotaxis assay across a polycarbonate membrane with 5-μm pores (Chemotaxicell-24; Kurabo, Osaka, Japan) using L1.2 transfectants expressing the specific receptor for chemokines. The culture supernatants of intact A549 cells, AdRGD-Luc-transfected A549 cells, and chemokine gene-transduced A549 cells were prepared. These samples and recombinant chemokines dissolved in the assay medium were added to a 24-well culture plate. Cells expressing specific receptors for CCL19 (L1.2/CCR7) or XCL1 (L1.2/XCR1) were suspended in the assay medium (1×10^6 cells) and placed in a Chemotaxicell-24 installed on each well. Likewise, parental L1.2 cells for these transfectants were prepared and added to the Chemotaxicell-24. Cell migration was allowed for 2 h at 37 °C in a 5% CO_2 atmosphere. The cells that migrated to the lower well were lysed and quantitated using a PicoGreen dsDNA quantitation reagent (Invitrogen, Tokyo, Japan). The data are expressed as mean±S.E. of the triplicate results and the migration activity was expressed in terms of the percentage of the input cells. Recombinant chemokines (mouse: mCCL19 and mXCL1) corresponding to each specific receptor (CCR7 and XCR1) were purchased from DakoCytomation (Kyoto, Japan) and used as a positive control.

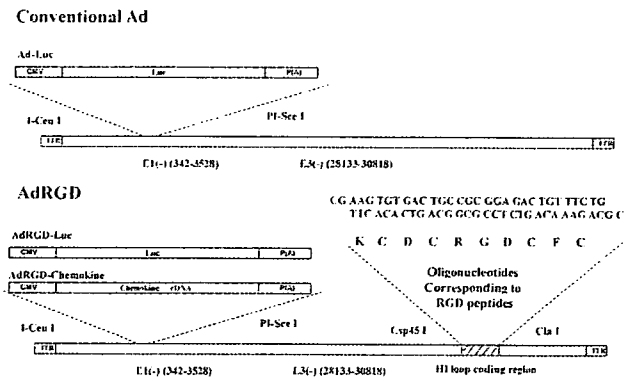

Fig. 1. Schematic Representation of Conventional Ad and AdRGD Used in This Study

Evaluation of Growth of OV-HM Cells Transfected with Chemokine-Encoding Adenovirus Vectors in Immunocompetent Mice OV-HM cells were transfected with AdRGD-mCCL19, AdRGD-mXCL1, or AdRGD-Luc as a control, at a MOI of 10 for 24 h. The cells were then harvested and washed with PBS three times and 1×10^6 cells were inoculated intradermally into the flank of B6C3F1 mice. An aliquot of the OV-HM cells infected with AdRGD-mCCL19, AdRGD-mXCL1 or AdRGD-Luc at a MOI of 10 were cultured for an additional 48 h, and cell viability was examined by MTT assay. For *in vivo* evaluation of OV-HM cell growth, tumor volume was calculated by measuring the length and width of the tumor, twice a week. The mice were euthanized when one of the two measurements was greater than 15 mm.

RESULTS

OV-HM Tumor Cells Transfected with Fiber-Mutant Adenovirus Vector Induced Higher Gene Expression Than That Induced by Conventional Vector To evaluate the gene transfection efficiency of the fiber-mutant adenovirus vector developed for this study, OV-HM cells were transfected with conventional adenovirus vector or fiber-mutant adenovirus vector at indicated particles/cell and luciferase activity was measured. The results shown in Fig. 2 demonstrated that luciferase gene expression induced by fiber-mutant vector was much higher than that induced by conventional adenovirus vector. For example, at 10000 VP/cell transfection, 16-fold greater gene expression was obtained in response to fiber-mutant vector than to Ad-Luc. This demonstrated that the insertion of the RGD peptide into the viral fiber enhanced transfection efficiency to OV-HM cells *via* the adenovirus vector.

Expression of Murine CCL19 and XCL1 by Transfection with Chemokine-Encoding Adenovirus Vector To

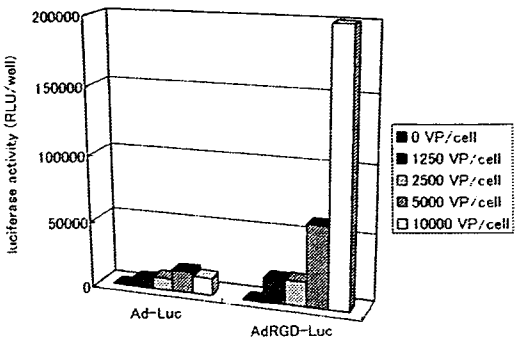

Fig. 2. Luciferase Expression by Ad-Luc or AdRGD-Luc Transfected OV-HM Cells

2×10^3 OV-HM cells were inoculated in a 96-well plate for 12 h, and were transfected with Ad-Luc (left) or AdRGD-Luc (right), respectively, at the indicated viral particles/cell for 1.5 h. The cells were then washed and incubated for another 48 h. After incubation, cells were collected and luciferase activity was measured. Data are presented as mean±S.E. of relative light units (RLU)/well determined from three experiments.

Table 1. Specific Chemoattractant Activity *in Vitro* Induced by Transfection of AdRGD-mCCL19 or AdRGD-mXCL1 into A549 Cells

	L1.2 % of input cells (mean±S.E.)	L1.2/XCR1 % of input cells (mean±S.E.)
Medium	0.2±0.0	0.1±0.0
10 nM mXCL1	0.3±0.0	9.2±0.8
A549	1.2±0.1	1.6±0.1
Luc/A549	1.5±0.0	2.0±0.2
mXCL1/A549	3.7±0.3	11.6±0.7

	L1.2 % of input cells (mean±S.E.)	L1.2/CCR7 % of input cells (mean±S.E.)
Medium	0.2±0.0	0.7±0.1
10 nM mCCL19	0.2±0.0	16.3±1.2
A549	1.2±0.1	2.0±0.1
Luc/A549	1.5±0.0	2.2±0.2
mCCL19/A549	2.5±0.1	8.2±0.5

Chemotaxis assay was performed using L1.2 cells expressing specific receptors for CCL19 (L1.2/CCR7) or XCL1 (L1.2/XCR1).

verify that the CCL19 and XCL1 produced by AdRGD-mCCL19 and AdRGD-mXCL1, respectively, were biologically functional, A549 cells were infected with the vectors for 2 h, and the culture supernatants were harvested after an additional 48 h. In the present study, human lung carcinoma A549 cells were used instead of murine tumor cells because of the very strong background chemotactic activity in the culture supernatant of the latter.[16] Using an *in vitro* chemotaxis assay, we investigated whether A549 cells transfected with each chemokine gene-carrying AdRGD could secrete chemokine protein in its biologically active form into culture supernatants. As shown in Table 1, the culture supernatants of A549 cells transfected with AdRGD-mCCL19 (mCCL19/A549) or AdRGD-mXCL1 (mXCL1/A549) could induce greater migration of cells expressing the corresponding chemokine receptors than those from intact A549 cells or A549 cells transfected with AdRGD-Luc (Luc/A549). The migration of L1.2 cells was not observed in wells containing recombinant chemokines, and only low-level migration was observed in culture supernatants from intact A549, Luc/A549, mXCL1/A549, and mCCL19/A549. These results demonstrated that all AdRGDs could deliver their encoded chemokine gene to target cells, and that transfected cells could secrete the chemokine protein, which maintained its original chemoattractant activity.

Anti-tumor Effect *in Vivo* by Transfection of Chemokine CCL19 into OV-HM Cells *via* Fiber-Mutant Adenovirus Vector OV-HM ovarian carcinoma cells transfected with 10 MOI of AdRGD-mCCL19, AdRGD-mXCL1 or AdRGD-Luc as the control vector, were intradermally inoculated into B6C3F1 immunocompetent mice to evaluate their effects on tumor growth *in vivo*. In the present study, 10 MOI of Ad vectors were chosen for transfection because that higher MOI induced the cytotoxicity of OV-HM cells (data not shown). As shown in Figs. 3A and B, the transfection of AdRGD-mCCL19 resulted in significant suppression of tumor growth, while that of AdRGD-mXCL1 did not show any difference from that with AdRGD-Luc. To exclude the possibility that the suppression of tumor cell growth by AdRGD-mCCL19 was due to the cytotoxicity of the adenovirus or chemokine, OV-HM cells transfected with AdRGD-mCCL19, AdRGD-mXCL1 or AdRGD-Luc were cultured for 48 h, and cell viability was measured by the MTT assay. The *in vitro* growth of the cells infected with these vectors was essentially identical to that of control cells (Fig. 3C).

DISCUSSION

Cytokines or chemokines encoded by a viral vector are currently regarded as intriguing options for cancer gene immunotherapy. Adenovirus vector, which shows high gene transduction efficiency and which can infect both dividing and non-dividing cells, is widely used as a carrier for gene therapy. It has been reported that the initial process of adenovirus infection involves at least two sequential steps. The first step is the attachment of the virus to the cell surface, which occurs by binding of the fiber knob to the Coxsackie virus and Adenovirus Receptor (CAR).[26,27] Following this, in the second step, the interaction between the RGD motif of the penton base with αv integrins, the secondary host-cell receptors, facilitates internalization through receptor-mediated endocytosis.[28,29] In other words, if the host cell surface lacks CAR, efficient gene transfer using a conventional adenovirus vector is difficult. Unfortunately, some malignant cells, including ovarian carcinoma, exhibit a resistance to adenovirus-mediated gene transduction due to low CAR expression on their surface. To overcome the low gene expression levels in CAR negative cells by adenovirus vectors, we constructed a fiber-mutant Ad vector with an integrin-targeting RGD peptide by a simple *in vitro* method.[20] The results of gene transfection *in vitro* (Fig. 2) demonstrated that OV-HM transfected using AdRGD-Luc carrying the luciferase gene significantly induced gene expression compared to that induced by the conventional Ad-Luc, suggesting that the recombinant adenovirus vector is a better option for cancer gene therapy.

We also inserted the murine chemokine cDNA of the CC family chemokine, CCL19, and C family chemokine, XCL1, into the E1 cassette of this fiber-mutant adenovirus vector, and AdRGD-mCCL19 and AdRGD-mXCL1 were developed. The expression of chemokine mRNA was reported pre-

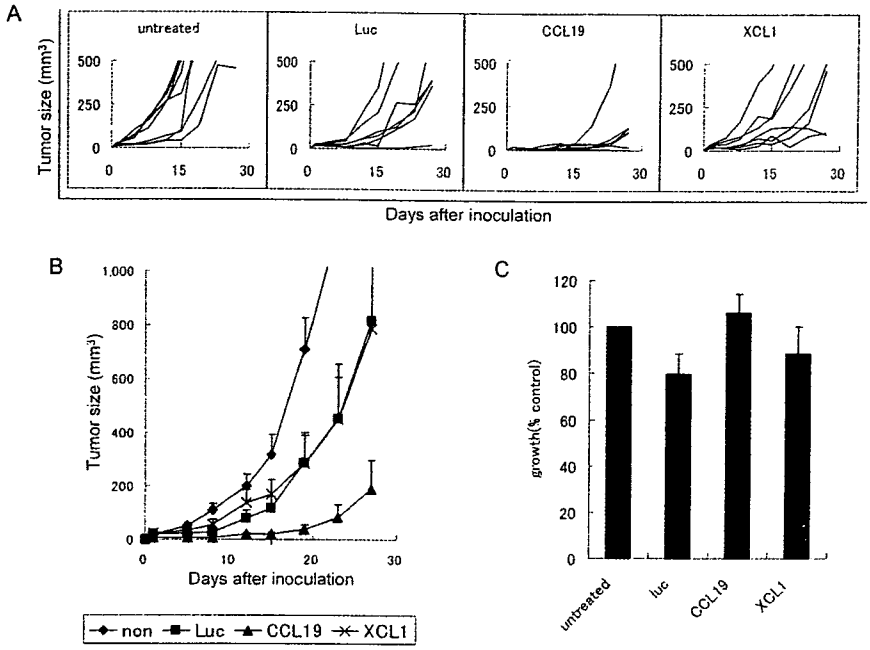

Fig. 3. Growth of OV-HM Tumor Cells in B6C3F1 Mice Transfected with Chemokine-Encoding Adenovirus Vectors

Mice were inoculated intradermally in the flank with 1×10^6 OV-HM cells (100 μl in RPMI 1640) at a MOI of 10 and with AdRGD-mCCL19 or AdRGD-mXCL1 for 24 h. Tumor volume was calculated after measuring the length and width of the tumor at indicated periods of time. Data are expressed as the mean±S.E. Intact OV-HM cells were used as control (untreated), and the OV-HM cells infected with AdRGD-Luc were inoculated into B6C3F1 mice for vector-control. Animals were euthanized when one of the two measured values were greater than 15 mm. At least six mice were used in each group. (A) Individual tumor size in each group and (B) average size in each group. (C) MTT assay results that evaluated the growth of chemokine-gene-transduced OV-HM cells *in vitro*. OV-HM cells were infected with AdRGD-mCCL19, AdRGD-mXCL1 or AdRGD-Luc at a MOI of 10 for 24 h, and then cultured for 48 h. Cell viability was examined by MTT assay. Data are expressed as the means±S.E. of triplicate results. Each of the analyses were performed at least three times.

viously.[30] A chemotaxis assay of chemokine-encoding vectors was conducted *in vitro* to evaluate the biological activity of these vectors. The results demonstrated that the produced protein in the culture supernatants of cells infected with these vectors could efficiently cause migration of the specific receptor-expressing cells (Table 1).

The C family chemokine, XCL1, has been widely used for cancer immunotherapy, but in general, XCL1 by itself did not induce notable anti-tumor effects, even though it is a chemoattractant for both T cells and NK cells.[31] The CC chemokine, CCL19, reportedly induces T cell and dendritic cell migration and exhibits tumor-suppressive effects in several mouse malignant cell models.[32,33] Hillinger *et al.* reported that intratumoral injection of recombinant CCL19 led to significant systemic reduction in tumor volumes. CCL19-treated mice exhibited remarkably increased infiltration of $CD4^+$ and $CD8^+$ T cell subsets as well as dendritic cells at the tumor sites. These cell infiltrates were accompanied by increases in several cytokines and chemokines such as IFN-γ, CXCL9, CXCL10, GM-CSF, and IL-12.[34] We have also shown that CCL19 and XCL1 elicited anti-tumor response, to some extent, through transfection into B16BL6 melanoma cells. But our study, which used eight chemokines to evaluate the anti-tumor effects in three tumor cell types, suggests that the tumor-suppressive activity of chemokine gene immunotherapy is very complicated and is greatly influenced by the type of tumor and activation state of the host's immune system.[30] Moreover, as we previously reported,[10] transfection with the chemokine CCL27 induced tumor-suppressive effects, whereas another chemokine, CX_3CL1, did not show any notable anti-tumor activity. However, both of these chemokines induced the accumulation of T cells as well as NK cells at the tumor site. Our results indicated that the distribution of immune cells that have migrated to the tumor and the angiogenic or angiostatic activity may play an important role in the anti-tumor response.

Several groups have reported much stronger anti-tumor activity when using chemokines as adjuvants with other agents.[35—39] In the present study, CCL19 could not induce complete tumor regression, but merely inhibited its growth. On other hand, remarkable anti-tumor activity could be obtained when XCL1 was combined with cytokines or tranfected into dendritic cells.[40,41] A recent report showed that combination of both XCL1 and CXCL10 can enhance the efficiency of adoptive T cell therapy for EG7 tumor cells *via* accumulation of effector T cells in tumor tissue.[42] Many factors are likely to influence the tumor-suppressive effects of chemokines, but the relatively weak anti-tumor activity and long-term immuno-protective effects of chemokines may be mainly related to the activation level of migrating immune cells. In other words, not only the accumulation but also the activation of immune cells migrating into tumors is important in cancer immunotherapy using chemokines. Therefore, combination therapy using both chemokines and cytokines will increase the anti-tumor effects and improve cancer immunotherapy.

Acknowledgements This study was supported by grants from the Ministry of Health, Labor, and Welfare of Japan and by Grants-in-Aid for Scientific Research on Priority Areas from the Ministry of Education, Culture, Sports, Science and Technology of Japan.

REFERENCES

1) Yoshie O., Imai T., Nomiyama H., *Adv. Immunol.*, **78**, 57—110 (2001).
2) Baggiolini M., *J. Intern. Med.*, **250**, 91—104 (2001).
3) Homey B., Muller A., Zlotnik A., *Nat. Rev. Immunol.*, **2**, 175—184 (2002).
4) Wang Q., Yu H., Zhang L., Ju D., Pan J., Xia D., Yao H., Zhang W., Wang J., Cao X., *J. Mol. Med.*, **80**, 585—594 (2002).
5) Strieter R. M., Polverini P. J., Arenberg D. A., Walz A., Opdenakker G., Van Damme J., Kunkel S. L., *J. Leukoc Biol.*, **57**, 752—762 (1995).
6) Huang S., Xie K., Singh R. K., Gutman M., Bar-eli M., *J. Interferon Cytokine Res.*, **15**, 655—665 (1996).
7) Laning J., Kawasaki H., Tanaka E., Luo Y., Dorf M. E., *J. Immunol.*, **153**, 4625—4635 (1994).
8) Maric M., Liu Y., *Cancer Res.*, **59**, 5549—5553 (1999).
9) Guo J., Wang B., Zhang M., Chen T., Yu Y., Regulier E., Homann H., Qin Z., Ju D. W., *Gene Ther.*, **9**, 793—803 (2002).
10) Gao J. Q., Tsuda Y., Katayama K., Nakayama T., Hatanaka Y., Tani Y., Mizuguchi H., Hayakawa T., Yoshie O., Tsutsumi Y., Mayumi T., Nakagawa S., *Cancer Res.*, **63**, 4420—4425 (2003).
11) Yoshida R., Nagira M., Imai T., Baba M., Takagi S., Tabira Y., Akagi J., Nomiyama H., Yoshie O., *Int. Immunol.*, **10**, 901—910 (1998).
12) Kellermann S. A., Hudak S., Oldham E. R., Liu Y. J., McEvoy L. M., *J. Immunol.*, **162**, 3859—3864 (1999).
13) Kennedy J., Kelner G. S., Kleyensteuber S., Schall T. J., Weiss M. C., Yssel H., Schneider P. V., Cocks B. G., Bacon K. B., Zlotnik A., *J. Immunol.*, **155**, 203—209 (1995).
14) Giancarlo B., Silvano S., Albert Z., Mantovani A., Allavena P., *Eur. J. Immunol.*, **26**, 3238—3241 (1996).
15) St George J. A., *Gene Ther.*, **10**, 1135—1141 (2003).
16) Wu H., Han T., Lam J. T., Leath C. A., Dmitriev I., Kashentseva E., Barnes M. N., Alvarez R. D., Curiel D. T., *Gene Ther.*, **11**, 874—878 (2004).
17) Okada N., Saito T., Masunaga Y., Tsukada Y., Nakagawa S., Mizuguchi H., Mori K., Okada Y., Fujita T., Hayakawa T., Mayumi T., Yamamoto A., *Cancer Res.*, **61**, 7913—7919 (2001).
18) Okada Y., Okada N., Nakagawa S., Mizuguchi H., Kanehira M., Nishino N., Takahashi K., Mizuno K., Hayakawa T., Mayumi T., *Cancer Lett.*, **177**, 57—63 (2002).
19) Hashimoto M., Niwa O., Nitta Y., Takeichi M., Yokoro K., *Jpn. J. Cancer Res.*, **80**, 459—463 (1989).
20) Mizuguchi H., Kay M. A., Hayakawa T., *Biotechniques*, **30**, 1112—1114 (2001).
21) Mizuguchi H., Koizumi N., Hosono T., Utoguchi N., Watanabe Y., Kay M. A., Hayakawa T., *Gene Ther.*, **8**, 730—735 (2001).
22) Mizuguchi H., Kay M. A., *Hum. Gene Ther.*, **9**, 2577—2583 (1998).
23) Maizel J. V., Jr., White D. O., Scharff M. D., *Virology*, **36**, 115—125 (1968).
24) Rosenfeld M. A., Siegfried W., Yoshimura K., Yoneyama K., Fukayama M., Stier L. E., Paakko P. K., Gilardi P., Stratfold-Perricaudet L. D., Perricaudet M., *Science.*, **252**, 431—434 (1991).
25) Crystal R. G., McElvaney N. G., Rosenfeld M. A., Chu C. S., Mastrangeli A., Hay J. G., Brody S. L., Jaffe H. A., Eissa N. T., Danel C., *Nat. Genet.*, **8**, 41—51 (1994).
26) Bergelson J. M., Cunningham J. A., Droguett G., Kurt-Jones E. A., Krithivas A., Hong J. S., Horwitz M. S., Crowell R. L., Finberg R. W., *Science*, **275**, 1320—1323 (1997).
27) Tomko R. P., Xu R., Philipson L., *Proc. Natl. Acad. Sci. U.S.A.*, **94**, 3352—3356 (1997).
28) Wickham T. J., Mathias P., Cheresh D. A., Nemerow G. R., *Cell*, **73**, 309—319 (1993).
29) Wickham T. J., Filardo E. J., Cheresh D. A., Nemerow G. R., *J. Cell Biol.*, **127**, 257—264 (1994).
30) Okada N., Gao J. Q., Sasaki A., Niwa M., Okada Y., Nakayama T., Yoshie O., Mizuguchi H., Hayakawa T., Fujita T., Yamamoto A., Tsutsumi Y., Mayumi T., Nakagawa S., *Biochem. Biophy. Res. Commun.*, **317**, 68—76 (2004).
31) Hedrick J. A., Saylor V., Figueroa D., Mizoue L., Xu Y., Menon S., Abrams J., Handel T., Zlotnik A., *J. Immunol.*, **158**, 1533—1540 (1997).
32) Nomura T., Hasegawa H., Kohno M., Sasaki M., Fujita S., *Int. J. Cancer*, **91**, 597—606 (2001).
33) Braun S. E., Chen K., Foster R. G., Kim C. H., Hromas R., Kaplan M. H., Broxmeyer H. E., Cornetta K., *J. Immunol.*, **164**, 4025—4031 (2000).
34) Hillinger S., Yang S. C., Zhu L., Huang M., Duckett R., Atianzar K., Batra R. K., Strieter R. M., Dubinett S. M., Sharma S., *J. Immunol.*, **171**, 6457—6465 (2003).
35) Narvaiza I., Mazzolini G., Barajas M., Duarte M., Zaratiegui M., Qian C., Melero I., Prieto J., *J. Immunol.*, **164**, 3112—3122 (2000).
36) Paillard F., *Hum. Gene Ther.*, **10**, 695—696 (1999).
37) Ruehlmann J. M., Xiang R., Niethammer A. G., Ba Y., Pertl U., Dolman C. S., Gillies S. D., Reisfeld R. A., *Cancer Res.*, **61**, 8498—8503 (2001).
38) Tolba K. A., Bowers W. J., Muller J., Housekneckt V., Giuliano R. E., Federoff H. J., Rosenblatt J. D., *Cancer Res.*, **62**, 6545—6551 (2002).
39) Dilloo D., Bacon K., Holden W., Zhong W., Burdach S., Zlotnik A., Brenner M., *Nat. Med.*, **2**, 1090—1095 (1996).
40) Emtage P. C., Wan Y., Hitt M., Graham F. L., Muller W. J., Zlotnik A., Gauldie J., *Hum. Gene Ther.*, **10**, 697—709 (1999).
41) Cao X., Zhang W., He L., Xie Z., Ma S., Tao Q., Yu Y., Hamada H., Wang J., *J. Immunol.*, **161**, 6238—6244 (1998).
42) Huang H., Xiang J., *Int. J. Cancer*, **109**, 817—825 (2004).

Vaccine Efficacy of Fusogenic Liposomes Containing Tumor Cell-Lysate against Murine B16BL6 Melanoma

Tomoaki YOSHIKAWA,[a,b] Naoki OKADA,*[,a,c] Masaki TSUJINO,[c] Jian-Qing GAO,[a,d] Akira HAYASHI,[a] Yasuo TSUTSUMI,[e] Tadanori MAYUMI,[f] Akira YAMAMOTO,[c] and Shinsaku NAKAGAWA*[,a,b]

[a] *Department of Biopharmaceutics, Graduate School of Pharmaceutical Sciences, Osaka University; 1–6 Yamadaoka, Suita, Osaka 565–0871, Japan:* [b] *"Creation of bio-devices and bio-systems with chemical and biological molecules for medical use", CREST, Japan Science and Technology Agency (JST); Tokyo 102–8666, Japan:* [c] *Department of Biopharmaceutics, Kyoto Pharmaceutical University; 5 Nakauchi-cho, Misasagi, Yamashina-ku, Kyoto 607–8414, Japan:* [d] *Department of Pharmaceutics, College of Pharmaceutical Sciences, Zhejiang University; 353 Yan-an Road, Hangzhou 310031, P. R. China:* [e] *National Institute of Biomedical Innovation; 7–6–8 Saito-Asagi, Ibaraki, Osaka 567–0085, Japan: and* [f] *Kobegakuin University; 518 Arise, Ikawadani-cho, Nishi-ku, Kobe 651–2180, Japan.*

Received August 23, 2005; accepted October 15, 2005; published online October 25, 2005

Recent advances in tumor immunology have facilitated the development of cancer immunotherapy targeting tumor-associated antigens (TAAs). However, because TAAs were identified in only a few types of human cancer, novel vaccine strategies that utilize tumor cell-lysate (TCL), including unidentified TAAs as an antigen source, are needed. Herein, we describe the utility of fusogenic liposomes (FLs) as TCL-delivery carriers for both *ex vivo* dendritic cell-based vaccination and *in vivo* direct immunization in the murine B16BL6 melanoma model. As a result, both *in vivo* direct immunization and *ex vivo* immunization induced anti-B16 melanoma prophylactic effects. *Ex vivo* dendritic cell (DC)-mediated vaccination strategy exert more potent anti-tumor effect than direct immunization. Our results suggest that this flexible system is a promising approach for the development of versatile cancer immunotherapy regimes.

Key words vaccine carrier; tumor cell lysate; liposome; melanoma

Early studies in mice demonstrated that tumor-specific cytotoxic T lymphocytes (CTLs) could control tumor growth and metastasis. The identification of T cell-recognizing tumor-associated antigens (TAAs) in human cancer, particularly in melanoma (*i.e.* MAGE, MART-1, gp100, tyrosinase, and TRP),[1,2] facilitated the development of cancer immunotherapy based on TAA-vaccination with adjuvants to elicit tumor-specific CTLs.[3] However, this immunological approach limits the application of this system only to certain cancer patients because TAAs are not yet identified for most of human cancers. Additionally, the expression levels of known TAAs that may be applicable for immunotherapy vary between tumor cells isolated from patients with cancer.[4] Therefore, it is very difficult to predict which TAA would generate an effective anti-tumor immune response that would make it appropriate for use as a vaccine component for a specific patient.

To overcome this limitation, several researchers have attempted to develop a vaccine strategy using tumor cell-lysate (TCL) as a possible source of TAA.[5] The use of TCL prepared from surgically removed tumors is a promising approach to induce a broader T cell-immune response not only to defined TAAs but also to unknown TAAs. In TCL-based cancer immunotherapy, the development of both an antigen-delivery system and an adjuvant that can efficiently prime and propagate CTLs specific for TAAs included in the TCL is required for achieving sufficient therapeutic effect. CTLs are activated by antigen-presenting cells (APCs), including dendritic cells (DCs), through the major histocompatibility complex (MHC) class I-restricted antigen presentation pathway. Peptides presented on MHC class I molecules are derived in most situations exclusively from endogenous antigens synthesized by cells. Antigens in the extracellular fluids fail to gain access to the MHC class I-pathway in most cells, although class I-presentation of endocytosed antigens also occurs in APCs under certain circumstances.[6,7] Therefore, if we can introduce the TAA-containing TCL directly into the cytoplasm, the TAAs would be definitively delivered to the MHC class I-antigen presentation pathway, much like cytoplasmic proteins.

Fusion active liposomes (fusogenic liposomes; FLs), which are composed of conventional liposomes (CLs) displaying Sendai virus-accessory proteins, retain membrane-fusion activity derived from Sendai-virus and efficiently introduce its contents into cytoplasm.[8] We have previously reported that direct antigen loading into cytoplasm by FLs is an efficient approach for enhancing antigen-specific CTL induction in mice.[9—11] In the present study, in order to evaluate the usefulness of FLs as antigen-delivery carriers for TCL-based cancer immunotherapy, we investigated anti-tumor efficacy of *ex vivo* vaccination using TCL-containing FLs (TCL/FLs)-pulsed DCs and *in vivo* direct TCL/FLs-immunization in the murine B16BL6 melanoma model.

MATERIALS AND METHODS

Cells and Mice B16BL6 cells, a C57BL/6-origin melanoma cell line, were grown in Eagle's minimum essential medium supplemented with 10% fetal bovine serum (FBS), and antibiotics. DC2.4 cells, a C57BL/6-derived DC line,[12] were generously provided by Dr. K. L. Rock (Department of Pathology, University of Massachusetts Medical School, Worcester, MA, U.S.A.), and were cultured in RPMI1640 medium supplemented with 10% FBS, 2 mM L-glutamine, 100 μM non-essential amino acid, 50 μM 2-mercaptoethanol, and antibiotics. CD8-OVA 1.3 cells, a T-T hybridoma against OVA+ H-2Kb,[13] were kindly provided by Dr. C. V. Harding (Department of Pathology, Case Western

* To whom correspondence should be addressed. e-mail: nakagawa@phs.osaka-u.ac.jp